Catalytic activity of P-cymene cracking on silica-alumina catalysts
by Baiwei Lin

A thesis submitted in partial fulfillment of the requirements for the degree of Master of Science in Chemical Engineering
Montana State University

Abstract:
Amorphous silica-aluminas are used as cracking catalysts in oil production. Many properties of silica-alumina materials affect the catalyst surface acidity, the types of active sites, the interfunction of acid sites, and the catalytic activity. Studying these properties will improve the fundamental development of amorphous acid catalysts. It will also be of interest to the bifunctional catalyst area.

The object of this study is to find relationships between catalytic cracking activity and alumina contents of catalysts, the correlation between cracking activity and different types of acid sites (Lewis acid site or Bronsted acid site), and the comparison of cracking activity and isomerization activity.

P-cymene was employed as a reactant to determine the extension of cracking reaction and catalytic activity over seven silica-aluminas with different alumina contents. Cracking activities measured at different temperatures gave the activation energy information and those measured at the same temperatures provided activity relations to acidity and alumina contents in the test catalysts.

P-cymene cracking reaction shows the maximum silica-alumina catalytic activity at about 25% alumina content. Cracking activity is found to be dominated mainly by Bronsted acid sites and by total acidity for low alumina-content catalysts. The similar activation, energies and rate constants for p-cymene cracking and o-xylene isomerization indicate that the two reactions are affected by the same kind of active sites and have reasonably similar reaction mechanisms. Bronsted acid sites definitely provide activity for both cracking and isomerization reactions. A mechanism for p-cymene cracking over silica-alumina catalysts is suggested.

CATALYTIC ACTIVITY OF P-CYMENE CRACKING ON SILICA-ALUMINA CATALYSTS

by

Baiwei Lin

A thesis submitted in partial fulfillment
of the requirements for the degree

of

Master of Science

in

Chemical Engineering

MONTANA STATE UNIVERSITY
Bozeman, Montana

May 1988

APPROVAL

of a thesis submitted by

Baiwei Lin

This thesis has been read by each member of the thesis committee and has been found to be satisfactory regarding content, English usage, format, citations, bibliographic style, and consistency, and is ready for submission to the College of Graduate Studies.

May 19, 1988
Date

John T. Sears
Chairperson, Graduate committee

Approved for the Major Department

May 19, 1988
Date

John T. Sears
Head, Major Department

Approved for the College of Graduate Studies

June 10, 1988
Date

Henry L. Parsons
Graduate Dean

STATEMENT OF PERMISSION TO USE

In presenting this thesis in partial fulfillment of the requirements for a master's degree at Montana State University, I agree that the library shall make it available to borrowers under rules of the library. Brief quotations from this thesis are allowable without special permission, provided that accurate acknowledgment of source is made.

Permission for extensive quotation from or reproduction of this thesis may be granted by my major professor, or in his absence, by the Dean of Libraries when, in the opinion of either, the proposed use of the material is for scholarly purposes. Any copying or use of the material in this thesis for financial gain shall not be allowed without my written permission.

Signature Baiwei Lin

Date May 19, 1988

ACKNOWLEDGMENTS

The author wishes to thank the faculty and staff of the Chemical Engineering Department at Montana State University for their guidance and assistance.

Thanks are extended to Dr. John Sears for his advice, encouragement, and support throughout the course of this research and thesis preparation.

The author also wishes to thank Dr. Johnny L. Golden for the use of catalysts which he prepared.

Thanks are also extended to Dr. Frank P. McCandless for the use of his equipment.

TABLE OF CONTENTS

TABLE OF CONTENTS--Continued

LIST OF TABLES

LIST OF FIGURES

LIST OF FIGURES--Continued

LIST OF FIGURES--Continued

ABSTRACT

Amorphous silica-aluminas are used as cracking catalysts in oil production. Many properties of silica-alumina materials affect the catalyst surface acidity, the types of active sites, the interfunction of acid sites, and the catalytic activity. Studying these properties will improve the fundamental development of amorphous acid catalysts. It will also be of interest to the bifunctional catalyst area.

The object of this study is to find relationships between catalytic cracking activity and alumina contents of catalysts, the correlation between cracking activity and different types of acid sites (Lewis acid site or Bronsted acid site), and the comparison of cracking activity and isomerization activity.

P-cymene was employed as a reactant to determine the extension of cracking reaction and catalytic activity over seven silica-aluminas with different alumina contents. Cracking activities measured at different temperatures gave the activation energy information and those measured at the same temperatures provided activity relations to acidity and alumina contents in the test catalysts.

P-cymene cracking reaction shows the maximum silica-alumina catalytic activity at about 25% alumina content. Cracking activity is found to be dominated mainly by Bronsted acid sites and by total acidity for low alumina-content catalysts. The similar activation energies and rate constants for p-cymene cracking and o-xylene isomerization indicate that the two reactions are affected by the same kind of active sites and have reasonably similar reaction mechanisms. Bronsted acid sites definitely provide activity for both cracking and isomerization reactions. A mechanism for p-cymene cracking over silica-alumina catalysts is suggested.

INTRODUCTION

Silica-alumina gel has long been used to make catalysts for cracking reactions in the petroleum industry. A lot of research studies have helped to elucidate characteristics of these catalysts, such as catalyst surface acidity, active site population and catalytic activity. But there are still many properties of silica-alumina materials which are not well understood.

Problems In This Area

In general, the silica-alumina catalyst has been observed to exhibit active sites which are suggested to be Lewis and Bronsted acidities with some apparent interconversion between the two types of sites. Some investigators believe that the cracking activity is only due to the Bronsted acid sites which are localized at the free hydroxyl groups on the surface. However, some cracking reactions have been found to correlate with the measurements of Lewis acidity. There is a disagreement over whether these active sites are Bronsted acid sites or Lewis acid sites.

Cracking reactions over a large range of alumina content in silica-alumina catalysts have been studied. With different alumina contents, the catalysts show variation of

acidities and cracking activities [7-18]. Bronsted acid sites and Lewis acid sites on silica-alumina surfaces have been distinguished by infrared spectroscopy with adsorption of ammonia and pyridine [9-15]. The maximum Bronsted-acid-site concentration occurs at about 25 percent alumina [14]. Similarly, measurements of some cracking reactions indicate a maximum silica-alumina catalyst activity at a bulk concentration of 15-25% alumina [18]. However, a satisfactory correlation between cracking activities and acidities has not been found. Some researchers suggest that the acid site strength seems to determine cracking activity more than acidity itself. Which one mostly determines the rate of cracking reactions is still unknown.

Some researchers formulated a simple mechanism of cracking based on a free-radical approach, which implies mostly thermal cracking [24]. Others suggested a carbonium ion mechanism in catalytic cracking, which could involve the Bronsted acidity [22]. Reactions involving carbonium ions include dealkylation, hydrogenation, isomerization, and polymerization. In the study of hydrocarbon cracking mechanism, the tracer technique using ^{14}C was adopted [23] and with the observed product distribution found in cracking reaction, it is still possible that Lewis acid sites directly or indirectly contribute activity to carbonium ion formation, e.g., to initiate a cracking reaction.

Motivation of This Work

Silica-alumina materials provide a perfect system for variation of acidity, ranging from very weak acids to very strong acids. The extensive background concerning silica-alumina makes the system ideal for a fundamental study of an amorphous solid surface. Though largely replaced by zeolites in the last few decades, amorphous silica-alumina catalysts are still used in the petroleum industry because of its better properties for heat transfer and diffusivity. Also, silica-alumina catalyst is a very important support for the metallic catalysts, such as a bifunctional hydrodesulfurization catalyst. This fundamental study will also be of interest to the area of such metallic catalysts.

J. Golden made a series of silica-aluminas with different alumina contents and studied their surface area, acid site density, the quantity of strong acid sites and catalytic activity for o-xylene isomerization [9]. It has been observed in his study that the strong acid amounts are in good agreement with literature reports for both commercial and research silica-aluminas, which shows the maximum acid site strength occurs at about 25 percent alumina; the activity measurements of o-xylene isomerization on these catalysts show the catalytic activity is mostly consistent with the acid-site strength distribution, that is the activity for o-xylene

isomerization is basically affected by strong acid-site acidity. The relation between catalytic activity of isomerization and Bronsted acidity indicates that Bronsted acid sites are primarily the active point for O-xylene isomerization.

The present work is a related study based on J. Golden's research and wishes to find the relationship between catalytic cracking activity and alumina content for the same series of catalysts. The question arises as to which type of acid site, Bronsted acid site or Lewis acid site, is more active for the p-cymene cracking reaction. Therefore a correlation of cracking activities with Bronsted acid strength as well as Lewis acid strength needs to be studied and is attempted in this work. A comparison of cracking activity with previous o-xylene isomerization activity will be done to see if there is a general activity dependence on acidity. Also, mechanisms of p-cymene cracking will be analyzed based on the product distribution.

Objectives

The purpose of this research is to contribute to the fundamental understanding of amorphous silica-alumina catalysts. The objectives are:

Examine the cracking activity of p-cymene on silica-alumina catalysts with different alumina contents and

determine a relationship between cracking activity and alumina content in the catalysts.

Correlate cracking activity of silica-alumina catalyst with acid site strength and implied acid site types (Bronsted or Lewis acid site).

Compare the cracking activity results to previous o-xylene isomerization activity on the same catalysts (obtained from J. Golden's research work) and discuss activity dependence on the acidity.

LITERATURE SURVEY

Silica-Alumina Surface Structure

Neither silica nor alumina is an active cracking catalyst, but a cogelled mixture of silica and alumina containing mainly silica is highly active. The incorporation of alumina into silica, even at very low concentrations results in the formation of surface sites. At least some of those sites must be Bronsted and/or Lewis acid sites [1].

Bronsted Acid Site

The OH groups terminating primary silica and alumina particles vary from weakly acids to strong acids (superacids) and show no cracking activity. The incorporation of trivalent aluminum ions into the silica surface produce surface OH groups having strong Bronsted acidity. The protonic acidity arises from the dissociative adsorption of H_2O on the aluminum ion:

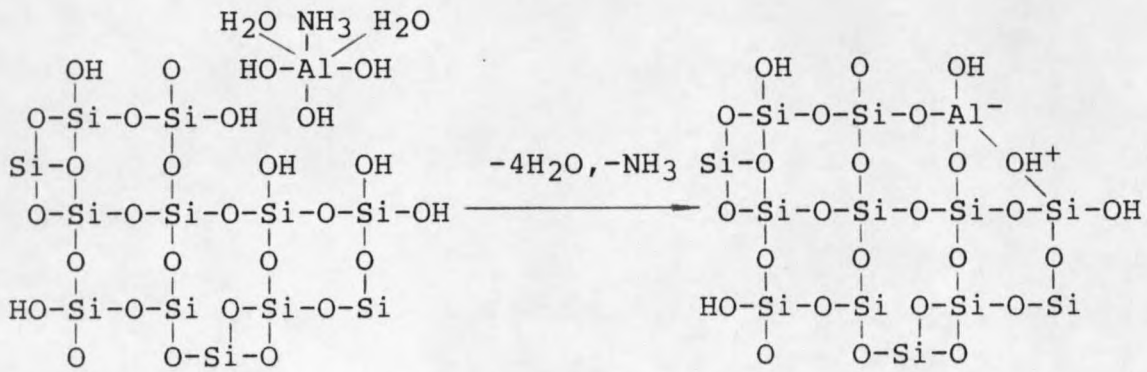

With the dissociation of water, alumina ions then tetrahedrally coordinate to oxide ions:

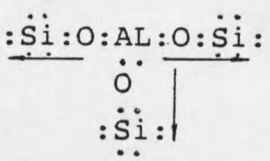

The strong electrophilic action of the aluminum ion is caused by the asymmetry of its position in the surface, where it is surrounded by quadra-valent silicon cations. Because of the asymmetry, the electronic charge is withdrawn from the aluminum ion to silica cations and make the alumina ion more positive. In this way aluminum ions develop a sufficiently strong field to acquire a hydroxyl group by splitting off hydrogen from water:

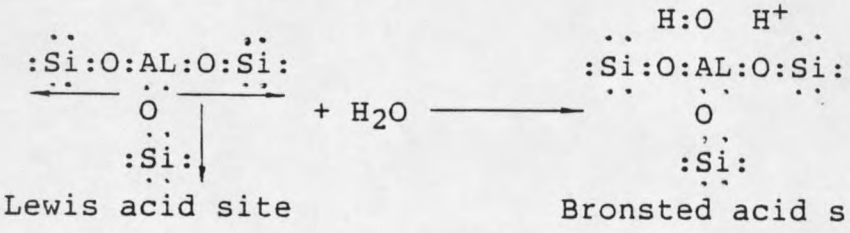

Lewis acid site Bronsted acid site

The structure of -Al-O-Si- group is strongly polarized by the asymmetry of aluminum ion which induces a strong acidity in the group.

Lewis Acid Site

When the silica-alumina surface is dehydrated by heating to high temperature, water is removed from the Bronsted site, exposing the aluminum ion with its electron-pair-

acceptor properties, thereby forming a Lewis acid site, as shown below:

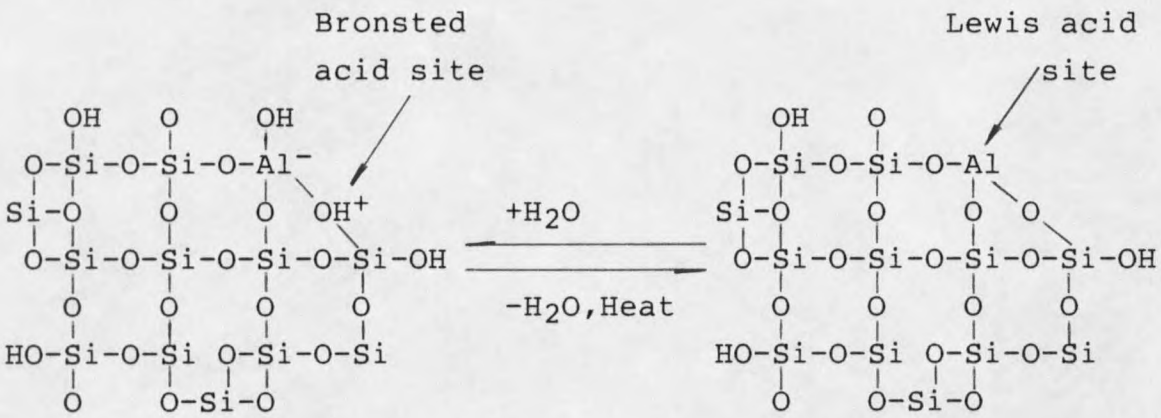

Alumina atoms acquire an additional electron pair to complete its bonding. Thus if the probe gas has additional electrons to interact with the Lewis site, it can share an electron pair with the aluminum atom. Water molecules may be coordinated at the Lewis acid site to provide a source of protons. Such Lewis acid sites are converted quantitatively to Bronsted acid sites upon the addition of water and reversibly back to Lewis acid sites upon heating. The dehydrated surfaces can show Bronsted acidity, Lewis acidity, or both, depending on the pretreatment conditions.

Acidities On Silica-Alumina Catalyst

Alumina does not show significant Bronsted acidity at any observed calcination temperature. With the adsorption of ammonia or pyridine, alumina has no infrared bands of NH_4^+

or pyridinium ion [2]. Although the OH groups on alumina do not show Bronsted acidity, alumina does show considerable Lewis acidity after calcination at relatively high temperatures. At elevated temperatures, dehydroxylation on the surface occurs and makes aluminum cations exposing an electron-pair-accepting nature after the OH groups have been removed. The concentration of the Lewis acid centers depends on treatment temperature [2,3].

Silica gel shows neither Bronsted nor Lewis acidity. Even at high temperature calcination, Lewis acidity is not observed [2,11]. From the infrared spectra of adsorbed pyridine, the Bronsted acidity of Si-Al materials increases with Si to Al ratio [4]. By introducing HF into silica gel, the Bronsted acid site is observed [5,6]. The Bronsted acid site appears because the charge induction through the oxygen-silica bridge to the fluorine atom, which increases the acidity of the neighboring O-H group. This effect occurs through the asymmetry of the surface and the strong charge-withdrawing characteristics of the fluorine. The electronic charge is pulled towards the fluorine and away from the O-H bond, making the O-H group a strong proton donor. This situation is similar to that involving an aluminum ion on the surface of a silica particle.

Fedorynska, et al. [7] investigated the acidity on silica-alumina surface as well as the concentration of surface hydroxyl groups. The catalysts were prepared by

hydrolysis of aluminum isopropoxide and ethyl ortho silicate. The catalyst surface areas are listed in Table 1.

Table 1. Specific Surface Area of Silica-Aluminas [7].

Al_2O_3 content (mol %)	surface area (m^2/g)
100	184
87	249
74	179
63	187
52	175
40	84
30	139
15	334
10	365
0	401

The distributions for amount and strength of acid sites were determined by titration in the presence of Hammett indicators. For a reaction of

$$H^+ + B = BH^+$$

The Hammett acidity function is defined as

$$H_0 = \log (a_{H^+} \times f_B/f_{BH^+})$$

where

a_{H^+} --- the thermodynamic activity coefficient of H^+

f_B --- the activity coefficient of a base

f_{BH^+} -- the activity coefficient of BH^+

The catalyst samples were suspended in benzene and the change of Hammett indicator color marked the end point of titration. Fig. 1 presents the distribution of acid sites at various strengths. The strongest acid sites are due to those

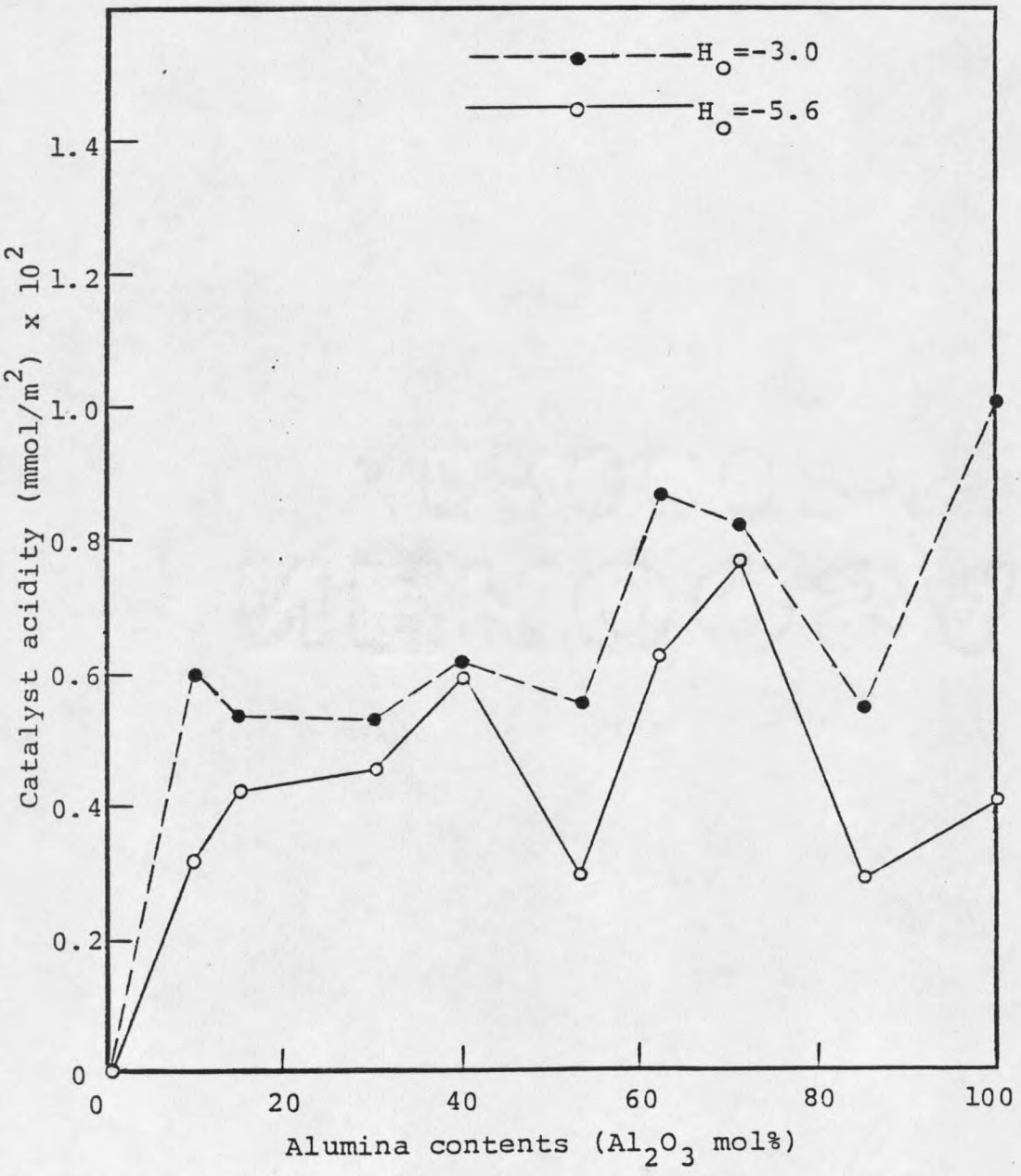

Figure 1. Variation of cumulative acidity as a function of alumina content [7] .

at acidity of H_0=-5.6. The sample containing small quantity of SiO_2 in Al_2O_3 exhibits the strongest acid properties.

For determination of OH groups, Fedorynska adopted Shima's method [8] involving titration with ethyl dichloroaluminum. Fig. 2 [7] demonstrated the amount of surface OH groups determined by the reaction with the organoaluminum compound. The concentration of OH groups varies nonuniformly with the composition of the catalysts.

J. Golden used triethylamine (TEA) as a gaseous base adsorbate to determine the acidities of silica-aluminas [9]. The TEA was used because of its stability against dissociation and its character as a sterically hindered Lewis base [10]. Therefore TEA is probably difficult to coordinate with surface Lewis acid sites and the strong Lewis acid sites can be discriminated from strong Bronsted acid sites.

The CAEDMON program [9] was used to calculate TEA adsorption energy distribution in Golden's work. Two site energies (weak site energy and strong site energy) were observed on the test material surfaces. Strong acidity against alumina content is shown in Fig. 3.

Distinguishing Two Types of Acid Sites

Extensive work reported in the literature shows that the activity of cracking catalysts results from the presence of acid centers on the catalyst surface. However, there is

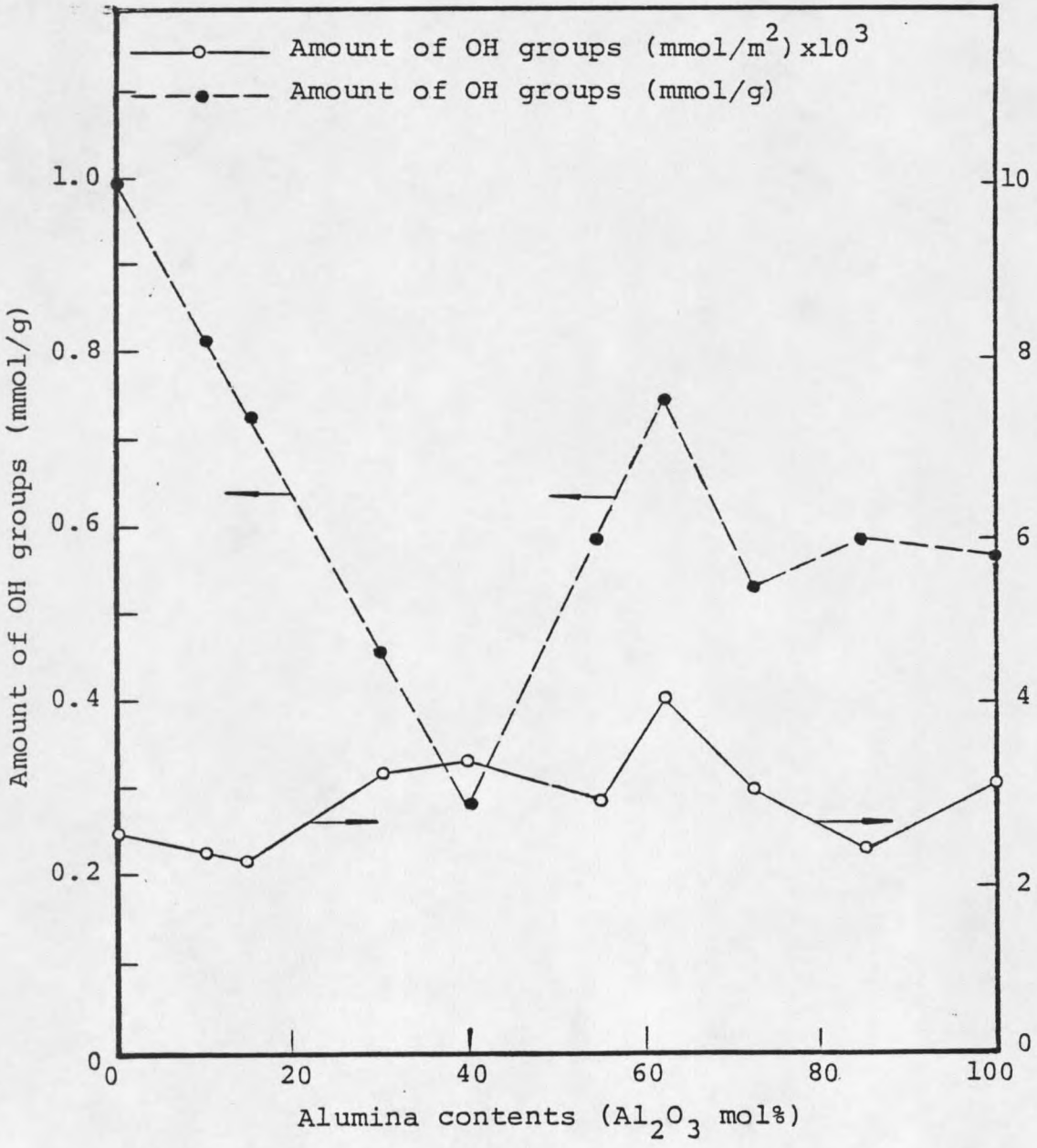

Figure 2. Variation of amount of OH groups as a function of alumina content [7].

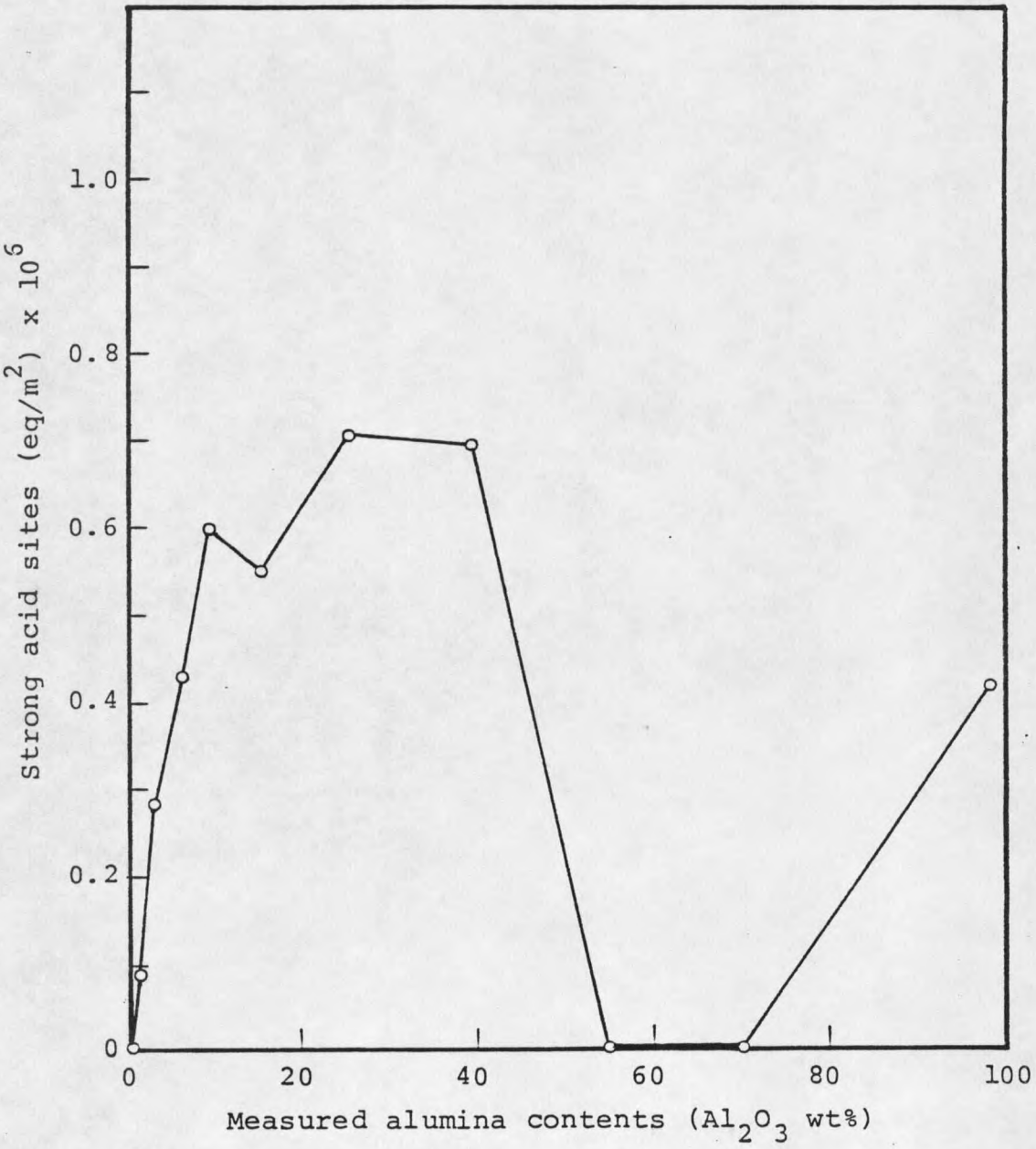

Figure 3. Relationship of the strong acidity measured from chemisorption isotherms to the measured alumina contents of the catalysts [9] .

disagreement over whether these acid centers are Bronsted or the Lewis acid sites. With the infrared spectra method, the two types of acid sites can be distinguished.

The Infrared Spectrum of Ammonia

In reacting with a Bronsted acid site, ammonia gains the available proton to form ammonium ion, converting the NH_3 configuration to NH_4^+. In reacting with a Lewis acid site, the nitrogen in ammonia contributes its free electron-pair to fill the vacancy of the acid, thus maintaining the NH_3 structure. Infrared spectrum offers a means of distinguishing the two adsorption forms. If NH_3 is indicated by the spectrum of chemisorbed ammonia, the presence of Lewis acid centers is shown. If NH_4^+ is observed, the presence of proton on the surface is shown.

Mapes and Eischans [11] utilized the infrared spectroscopy to determine the types of acid sites of silica-alumina with the chemisorption of ammonia. The characteristic adsorption bands for both NH_3 and NH_4^+appear in the spectrum. It indicated that both Bronsted and Lewis acid sites exist on the surface. Most of the acid centers were of the Lewis type, where the unshared electron-pair of the nitrogen atom fills the electron-pair vacancy of alumina.

The same method to determine type of acid sites was also adopted by Basila and Kantner [12]. The studied catalyst contained 25% Al_2O_3 by weight on a dry basis and had a

surface area of 430 m^2/g. From the relative intensities of the NH_3 and NH_4^+ bands, the ratio of Lewis to Bronsted acid sites was found to be 4:1. The result of this study indicated that all of the primary acid sites on a silica-alumina are of the Lewis type centered on active surface aluminum atoms, and apparent Bronsted sites are produced by a second-order interaction between the molecules chemisorbed on a Lewis site and a nearby surface hydroxyl group.

Bourne et al.[13] identified acid sites on two types of silica-aluminas. The two catalysts consisted of low concentration (<1.4 wt%) of aluminum atoms. It was found that dehydrated alumina-silica contained only Lewis sites and that hydrated alumina-silica contained only Bronsted acid sites. Addition of water to dehydrated alumina-silica converts part of the Lewis acid sites to Bronsted acid sites.

The Infrared Spectrum of Pyridine

By using gaseous base adsorption, infrared spectroscopy has ability to distinguish between Lewis and Bronsted acid sites. Pyridine can coordinatively bond to Lewis acid sites or can associate with Bronsted acid sites as the pyridinium ion. These two adsorbed species have different infrared absorption bands. The amount of either acid type can be determined from the absorption band intensities.

J.A. Schwarz [14] used this infrared technique along with a standard titration technique to determine the number

of Lewis and Bronsted acid sites. The acidities were determined both before and after water exposure to the catalysts. This modified titration technique was applied to a series of experimental silica-alumina catalysts from pure silica to pure alumina. The silica-aluminas were prepared by mixing desired amounts of $AlCl_3$ and tetraethylortho-silicate in methanolic solution. Samples were calcined at 500^0C. The total number of acid sites and the number of Lewis and Bronsted acid sites were determined as a function of the silica content of the catalysts. The results are summarized in Table 2.

Table 2. Acidities of SiO_2-Al_2O_3 From IR Results [14].

apparent content Al_2O_3	condition	Lewis acidity (μmoles/g)	Bronsted acidity (μmoles/g)	Total (μmoles/g)
100%	before H_2O	602	0	602
	after H_2O	131	0	131
90%	before H_2O	600	0	600
	after H_2O	147	0	147
75%	before H_2O	627	0	627
	after H_2O	164	0	164
50%	before H_2O	333	79.5	412
	after H_2O	89	332	421
25%	before H_2O	226.5	119.3	345.8
	after H_2O	104.4	245	349.4
10%	before H_2O	224	127	351
	after H_2O	128	219.5	347.5
0%	before H_2O	0	0	0
	after H_2O	0	0	0

Other Surface Spectroscopies

With the adsorption of amines on silica-alumina surface, the ^{13}C-NMR spectra can be used to estimate the concentration of the surface proton acids.

Gay and Liang [15] used ^{13}C-NMR spectra technique to study the surface acidities of SiO_2, Al_2O_3 and mixed silica-alumina catalysts. On SiO_2, only weak interactions with surface hydroxyls are observed. On Al_2O_3, much stronger interactions are observed. There is very little protonation of the corresponding amines in acids. It is shown that the strong acid site on Al_2O_3 are sterically hindered. On silica-alumina, protonation is observed. It is due to Bronsted acidity.

Bremer et al.[16] studied sodium poisoning by using ESR spectroscopy, infrared spectroscopy and deuterium exchange. They concluded that silica-alumina catalysts have a variety of strong Bronsted and Lewis acid sites. The strongest Bronsted acid sites are poisoned first by sodium.

Surface structure defects in silica-alumina catalyst have been determined by using radial electron distribution and X-ray fluorescence spectroscopy [17]. The conclusion is that Bronsted acid sites occur when aluminum cations tetrahedrally coordinate to oxide ions at the ratio of $Al_2O_3/(Al_2O_3+SiO_2)$ less than 1 in catalysts. At alumina contents greater than 50 wt%, silicon ions in a perturbed tetrahedral provided Lewis acidity. It is consistent with

the results of Table 2 in which high Lewis acidity is observed at high alumina percentages.

Catalytic Activity

Pure silica, which shows neither Bronsted nor Lewis acidity, is inactive for catalytic cracking, whereas silica-alumina is active. Alumina, which has only Lewis acidity, was shown by Hall et al. [6] to be very active in cracking but to deactivate almost immediately, which indicates that Bronsted acidity is necessary for the maintenance of activity.

Holm and Clark [18] investigated the activities on eleven silica-alumina gels ranging from pure alumina to pure silica. The test materials were produced by coprecipitation from solutions of sodium silicate and sodium aluminate [19]. Surface areas and other properties for those silica-aluminas are given in the Table 3 [20].

Table 3. Properties of Silica-Alumina Catalysts [20].

composition* (SiO_2 %)	Na (%)	surface area (m^2/g)	protonic acidity ($\mu eq/m^2$)
0	<0.002	303	0
8	0.003	292	0.14
15	0.008	358	0.18
40	0.18	309	0.48
55	0.17	249	0.99
70	0.22	296	1.55
82	0.036	397	1.78
90	0.010	510	1.45
95	0.004	562	1.18
98	0.003	564	0.63
100	0.026	344	0.27

* Composition is apparent silica content.

The octane cracking tests were carried out at 550^{0}C, and o-xylene isomerization was conducted at 350^{0}C. Propylene polymerization were carried out in a rising temperature reactor, the temperature for maximum conversion was 210^{0}C for all catalysts [18]. In Fig. 4, the conversion per square meter of catalyst surface for each of three reactions is plotted against catalyst composition. All of the reactions behave similarly. Conversions show maxima between 70% and 85% silica. They can be related to the differential entropies (S_T) of adsorbed ammonia on the same series catalysts. Fig. 5 shows that S_T isotherms start at low values of coverage, rise rapidly, and then fall if adsorbate-adsorbate interaction occurs. The maximum value attained by S_T is a measure of maximum mobility of adsorbates. The curve in Fig. 5 shows the same pattern as the curves in Fig. 4. It can be inferred that the three reactions took place most rapidly where the mobility of adsorbate is high and desorption of products is rapid.

Catalytic activity for carbonium-ion reactions has been correlated with catalyst surface acidity in several instances. Fig. 6 shows the linear relationship between isobutane cracking activity and the Lewis-acid-site concentration on the surface of silica-alumina catalyst [21]. The correlation suggested that Lewis acid site are necessary for abstracting a hydride ion from isobutane to

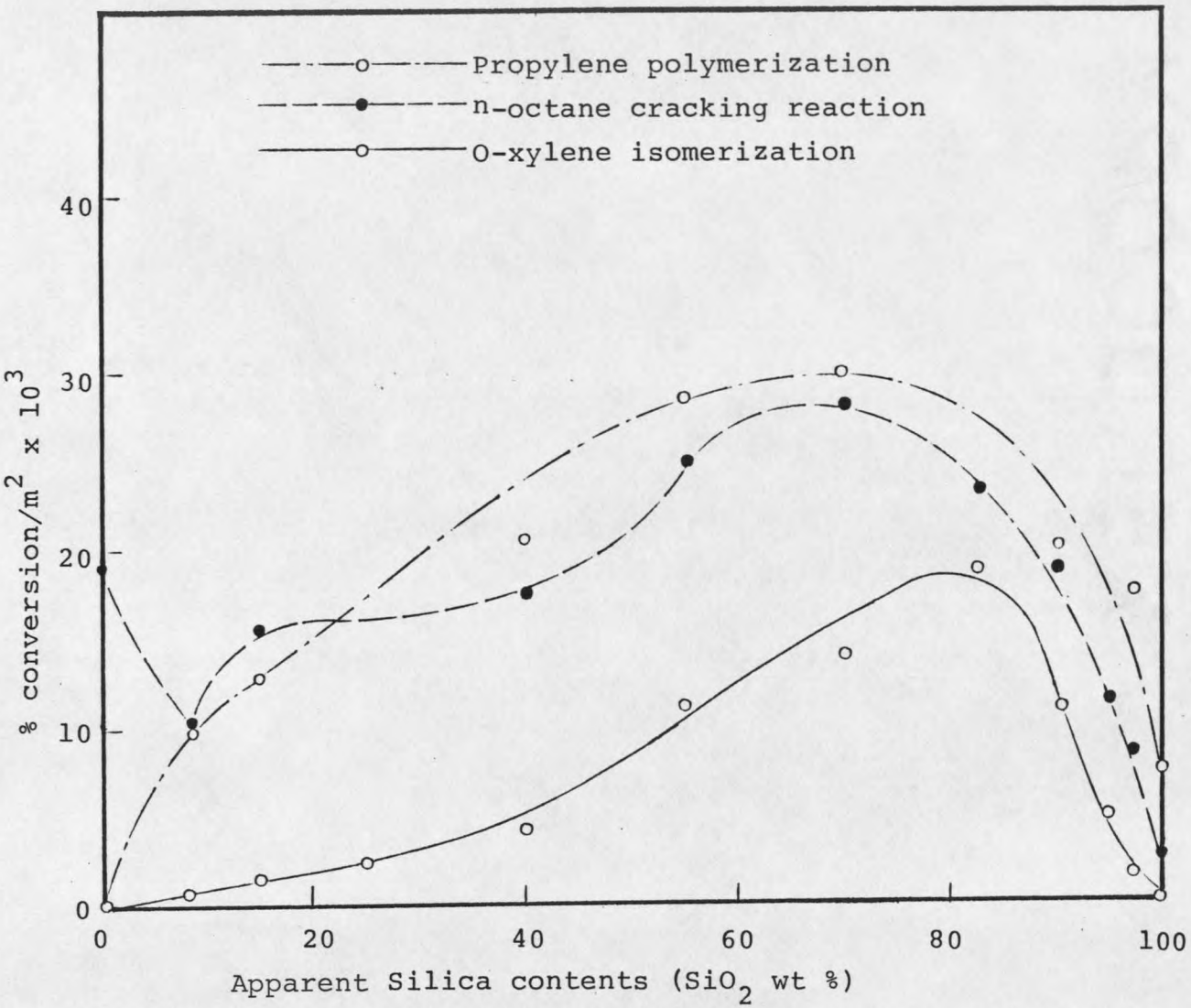

Figure 4. Relationship of catalytic activities to silica contents of silica-alumina catalysts [18].

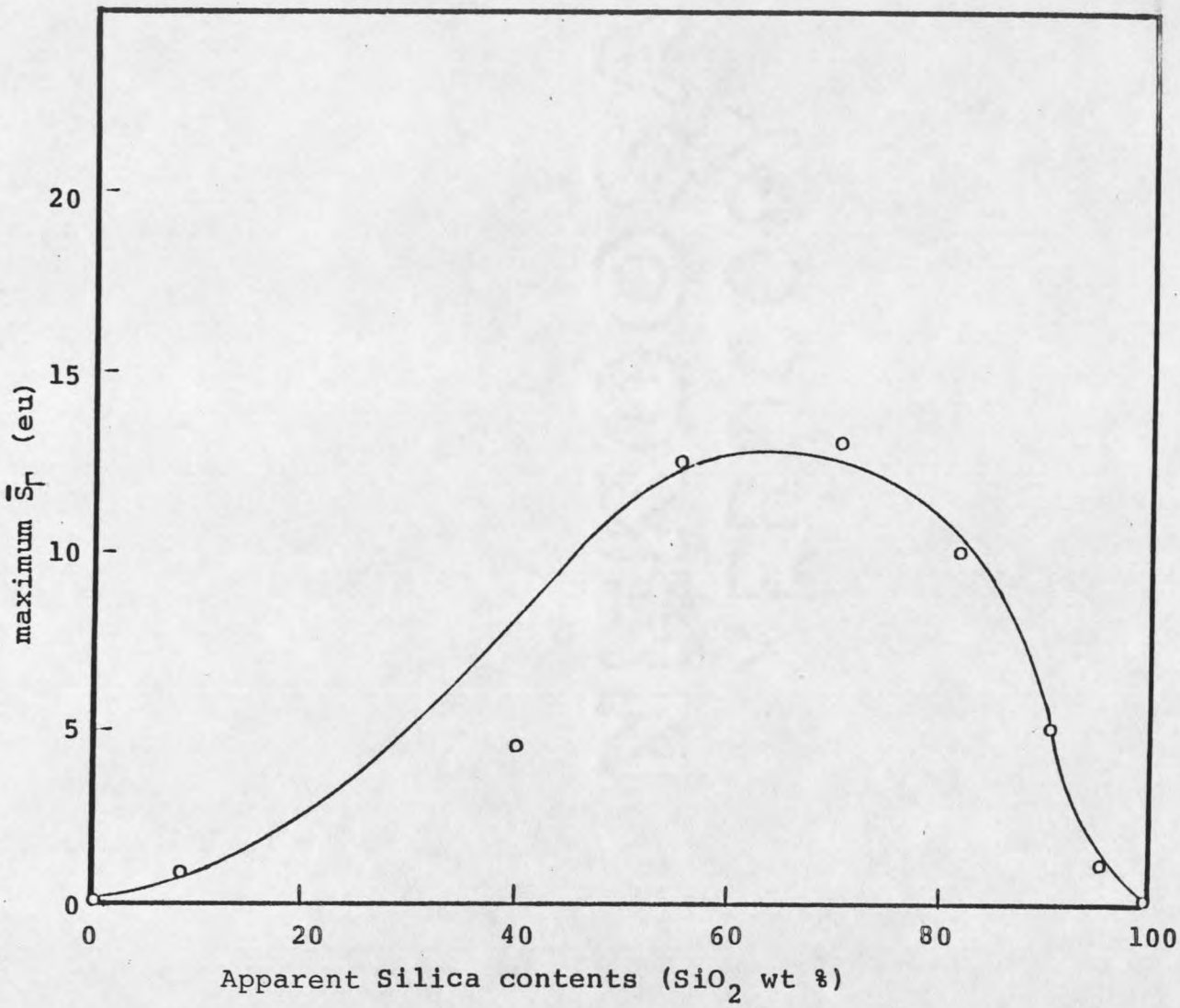

Figure 5. Relationship of entropies (relative maximum mobility) of adsorbed ammonia to silica contents of silica-alumina catalysts [18].

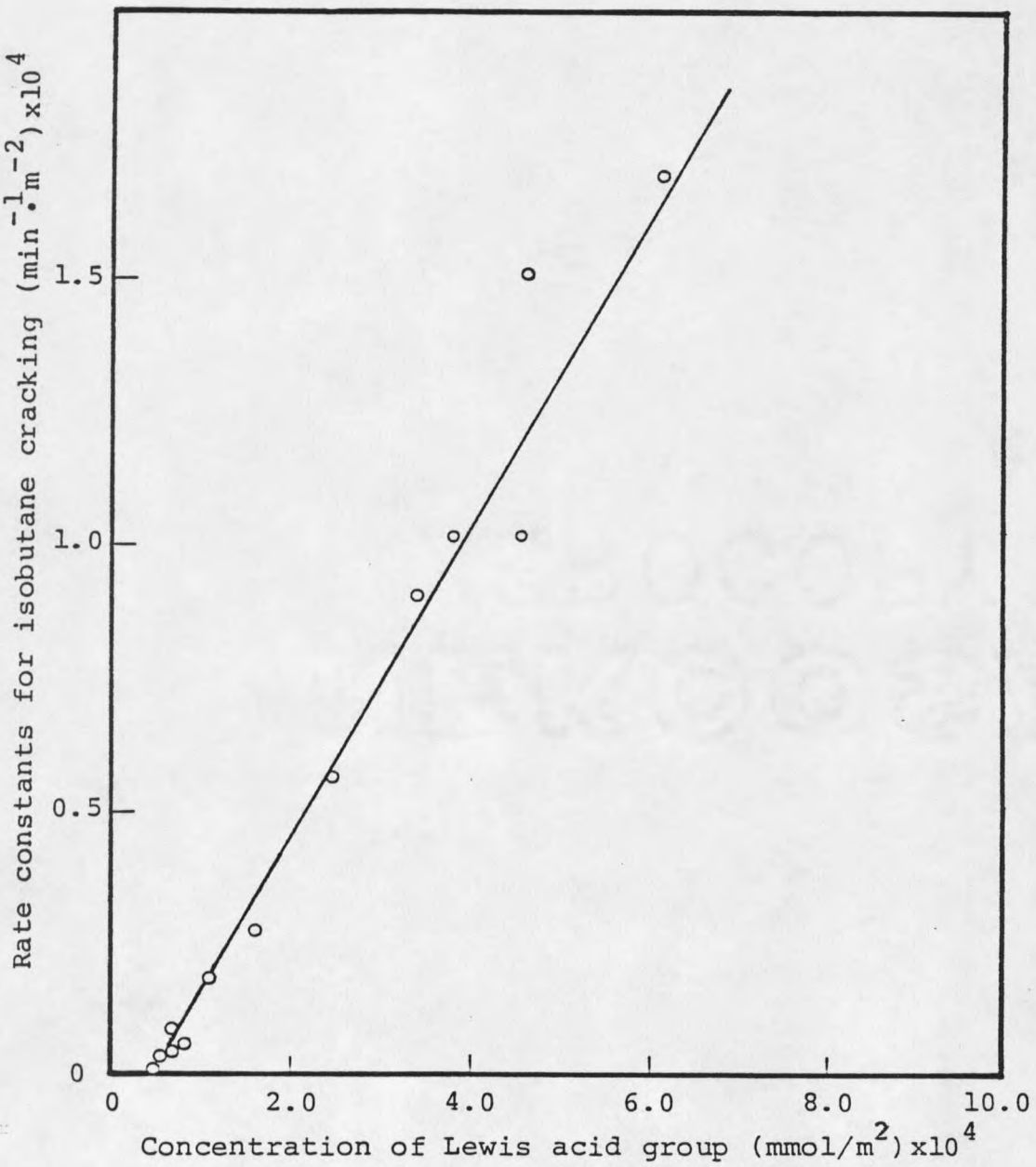

Figure 6. Isobutane cracking activity of silica-alumina catalysts of varying Lewis acid group concentration [21].

initiate the cracking reaction, but it is still possible that the Lewis acid sites operate indirectly by enhancing the acidity of adjacent Bronsted sites through charge withdrawal from the O-H bond.

J.A. Schwarz [14] compared the measured Bronsted acidity with catalytic activity. Fig. 7 compares the Bronsted acidities obtained from the titration technique with those activities obtained by Holm and Clark [18] who used a standard test reaction (the isomerization of o-xylene) to discuss the acidity dependence on silica-alumina catalysts. As can be seen, there is an excellent correlation between the catalytic activity of the silica-alumina catalyst and the "physical acidity" as determined by the modified pyridine titration. It is clear that the Bronsted sites play a major role in the isomerization.

J. Golden measured the activities of o-xylene isomerization on a series of silica-alumina gels [9]. The reactions were run in a continuous Berty reactor at 300^0C. Fig. 8 presents the surface area specific reaction rate for o-xylene isomerization against alumina content of the catalysts. The samples containing 0%, 54%, 79%, and 96% Al_2O_3 show no activity in o-xylene isomerization. The isomerization reaction over silica-alumina catalysts has been reported as a first-order reaction [28,29].

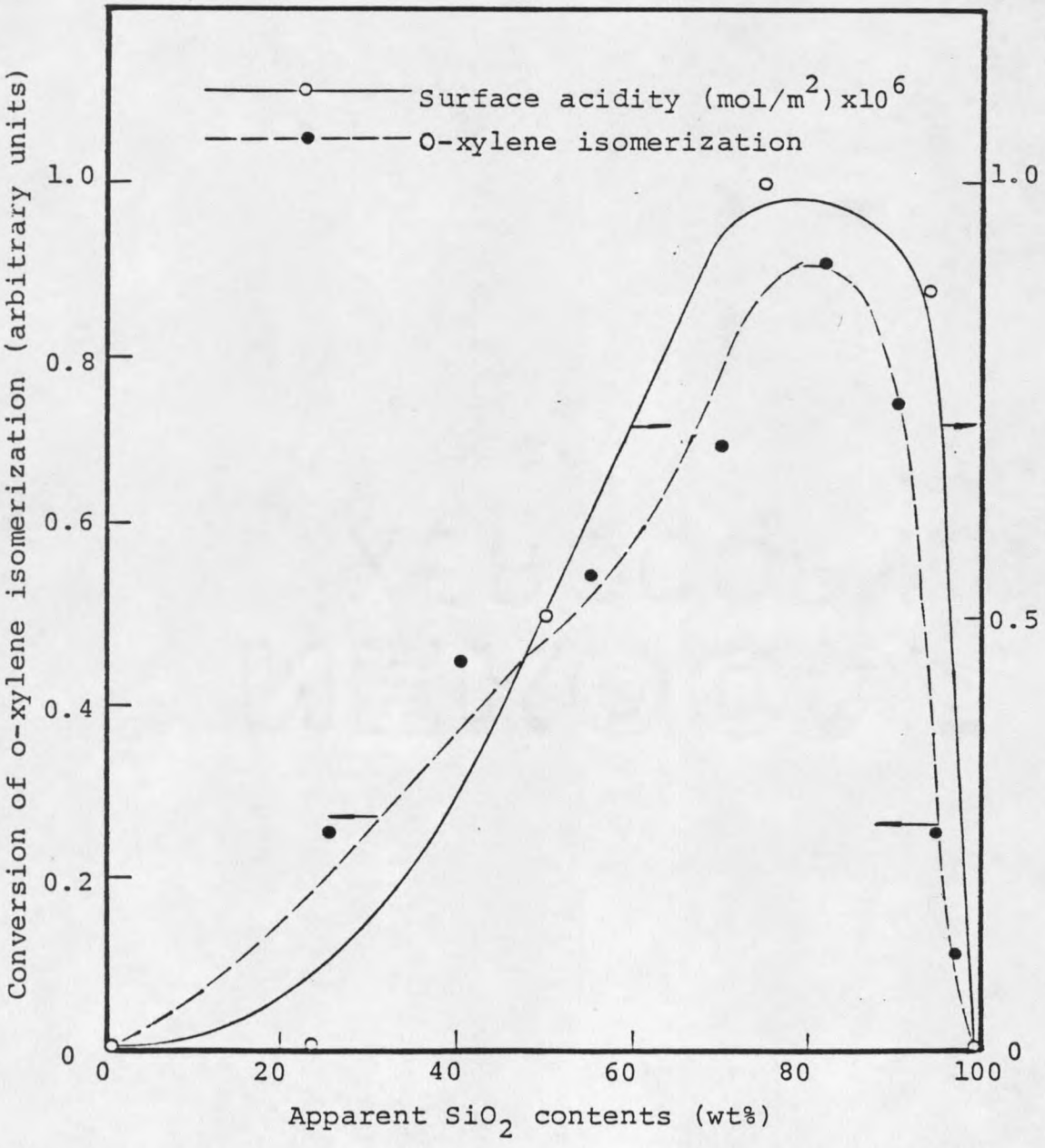

Figure 7. Comparison of the measured Bronsted acidity with catalytic activity from the data of Holm and Clark [14,18].

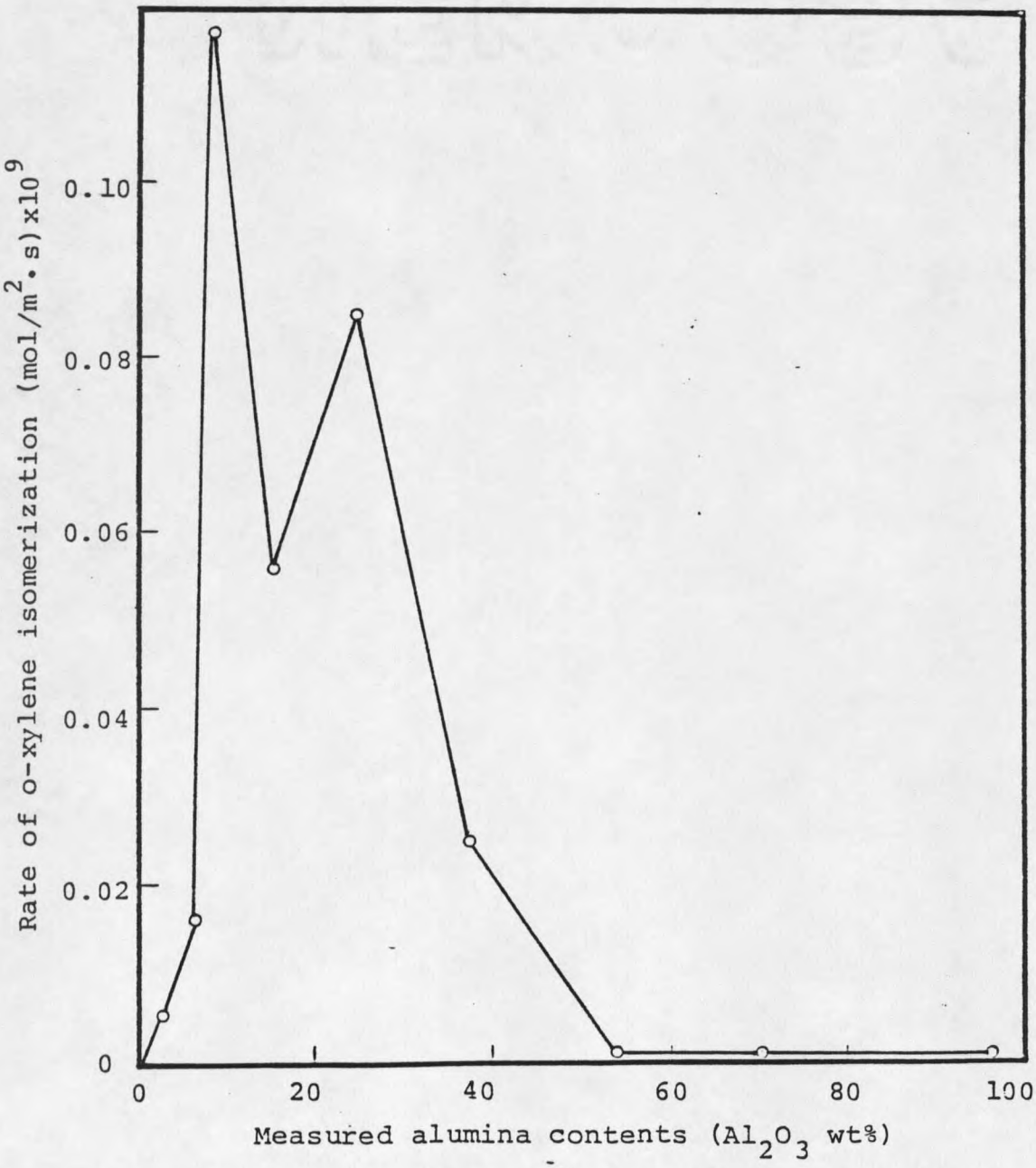

Figure 8. Relationship of the o-xylene isomerization rate at 300°C to the measured alumina contents of the test catalysts [9].

P-cymene Cracking Mechanism

Tracer techniques have been used in studying the mechanisms of hydrocarbon reactions. The technique of formulating a mechanism based on its product distributions is also a general method [22].

Hightower and co-workers [23] adopted the ^{14}C tracer technique to study the mechanisms of cracking reaction of several hydrocarbons. From the knowledge of the products of p-cymene cracking, it is possible to formulate a simple mechanism of cracking based on free radical [24] or a carbonium ion mechanism occurred on acidic catalysts [25,26].

During thermal cracking, the major products were toluene and saturated gaseous hydrocarbons [24]. Its formation may be explained on the basis of a free-radical mechanism as

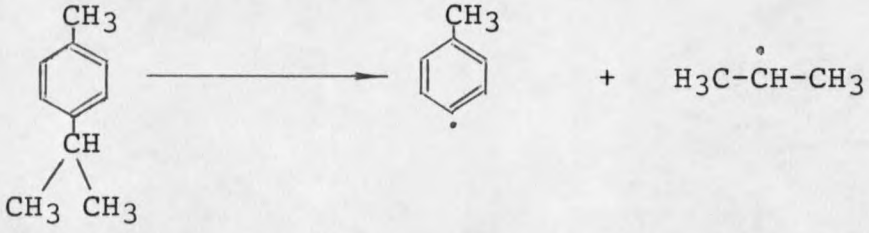

The question arises as to why the pattern should not be

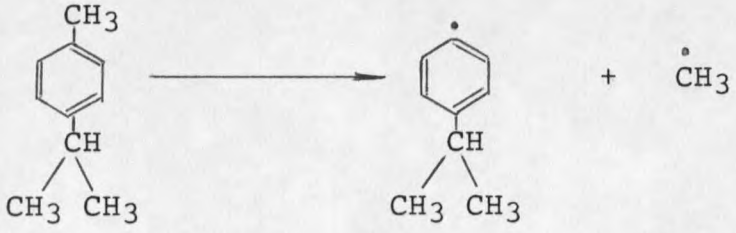

Usually it is the heavier side chain that splits more easily than the shorter one because the larger hydrocarbon groups have more steric effects and lower stability during the reaction.

Janardhan and Rajesuari [22] studied the p-cymene cracking reaction over a silica-alumina gel. Toluene, xylene, and cumene were the major products in p-cymene cracking reaction. The efficiency of the catalyst and the optimum temperature for effective cracking were decided on the basis of p-cymene conversion.

Cracking was carried out using gels aged at different temperatures. In each case the temperature of cracking was maintained the same as the aging temperature of the gel, subject to a maximum of 500^0C. The results of p-cymene cracking are represented in Table 4.

Table 4. Product From P-cymene Cracking [22].*

Aging Temp. of catalyst	200^0C	300^0C	400^0C	500^0C
Temp. of cracking	200^0C	300^0C	400^0C	500^0C
gaseous products:				
olefins	-	-	4	19
hydrogen	-	-	-	4
saturated hydrocarbons	-	10	11	13
liquid distillate:				
C_7 fraction	-	15	30	32
C_8 fraction	-	-	2	10
C_9 fraction	-	-	-	15
unreacted p-cymene	98	72	45	2

* The values indicate the weight percentages.

Among the products of catalytic cracking, there is predominance of the C_7 fraction and presence of the C_8, C_9 fractions. Also, the quantity of unsaturated gaseous products is more than those in thermal cracking. Moreover, catalytic cracking yields fractions which are more uniformly distributed over C_7-C_9 range. The probable steps of cracking have been outlined as follows:

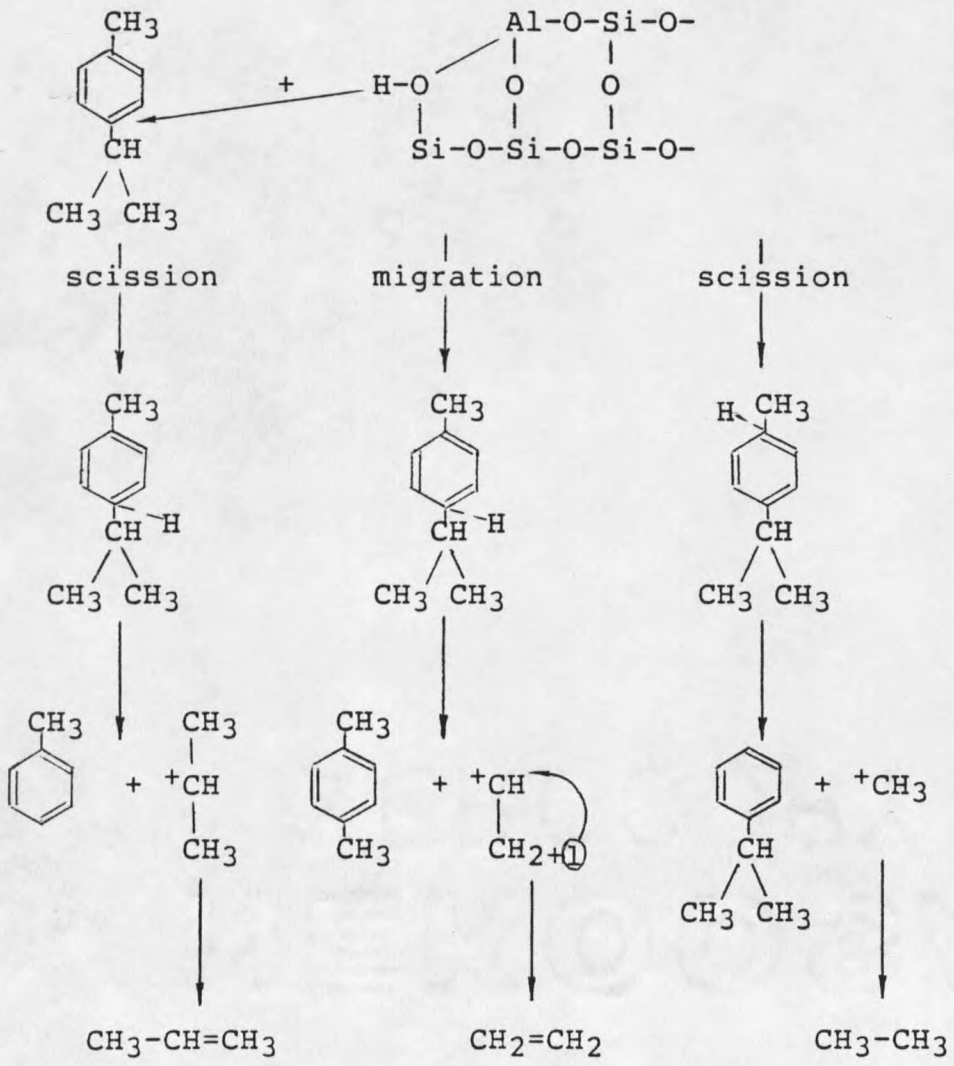

EXPERIMENTAL

Catalysts For Cracking Reaction

For the reason of comparison of the catalytic activities for both cracking and isomerization, the same silica-aluminas made by J. Golden were used in this research. These silica-aluminas thus are the same materials used in his o-xylene isomerization studies.

The catalysts were prepared by the following procedure:

A desired amount of aluminum nitrate solution was pipetted into the silica sol while stirring. The mixture was adjusted to pH 6 with 2N ammonium hydroxide, where it became a hydrogel.

The hydrogel was filtrated, washed, and placed in a drying oven at 110^0C over night. The dryed silica-alumina material was then ground. Particle sizes between 140 and 325 mesh were chosen for the available catalysts.

The catalysts were made as 5-mm diameter by 3-mm thick pellets. The pellets were pressed from silica-alumina particles and were calcined at 500^0C for four hours. At this point the pellets were considered as catalysts.

The physical properties of these silica-alumina catalysts are listed in Table 5 [9]. Surface areas of the catalysts were measured by their nitrogen adsorption at

liquid nitrogen temperature. The strong acidities of the catalysts were obtained by CAEDMON program for triethylamine (TEA) chemisorption on silica-alumina surfaces at 300^0C.

Table 5. Properties of Catalysts [9].

sample	measured Al_2O_3 (wt%*)	surface area by BET (m^2/g)	acidity by CAEDMON (meq/m^2)	coverage by TEA (m^2/m^2)	acid site density ($sites/m^2$)
A-3	2.86	426	2.85×10^{-4}	0.065	1.71×10^{17}
A-7	6.10	338	4.30×10^{-4}	0.098	2.59×10^{17}
A-10	8.50	285	5.93×10^{-4}	0.140	3.57×10^{17}
A-18	15.0	138	5.44×10^{-4}	0.120	3.28×10^{17}
A-26	24.5	174	7.09×10^{-4}	0.160	4.27×10^{17}
A-44	38.7	198	6.96×10^{-4}	0.160	4.19×10^{17}
A-65	54.1	7	-	-	-
A-88	70.4	68	0	0	0
A-100	96.6	202	4.42×10^{-4}	0.10	2.66×10^{17}

* Al_2O_3 content measured by atomic absorption.

Reactant For Cracking Reaction

Toluene, xylene, p-cymene, decalin, and tetralin have been used in cracking reactions for catalytic activity study by many researchers. These aromatic hydrocarbons show good characters for their ease of break at the side chains and for the simple specification of their products.

Janardhan and Rajesuari [22] studied cracking reactions

with several aromatic hydrocarbons. Among those reactants, p-cymene proved to be the best one because of its easy analysis for products. P-cymene was then employed to study the efficiency of the catalysts in cracking reaction. Another reason for using p-cymene as a cracking reactant is that there are similarities between cymene and xylene: p-cymene molecular structure is close to o-xylene molecular structure; also the products in p-cymene cracking may include xylene (o-xylene, m-xylene, and p-xylene).

The comparison between p-cymene cracking and o-xylene isomerization thus is relevant to explain the properties of silica-aluminas.

Equipment For Cracking Reaction

Fig. 9 shows the apparatus used here for cracking investigation. The process includes four sections: the saturator, the reactor, the analytical system and the heating system.

Saturator

The reactant p-cymene was delivered to the reactor at its saturated vapor pressure. P-cymene has a very low vapor pressure at room temperature (2 mmHg at 25^0C). In order to provide enough p-cymene vapor to the reactor, the saturator temperature must be increased as high as 200^0F (93.33^0C). At this condition p-cymene saturated vapor pressure is 51 mmHg. This process was accomplished with the use of a metal

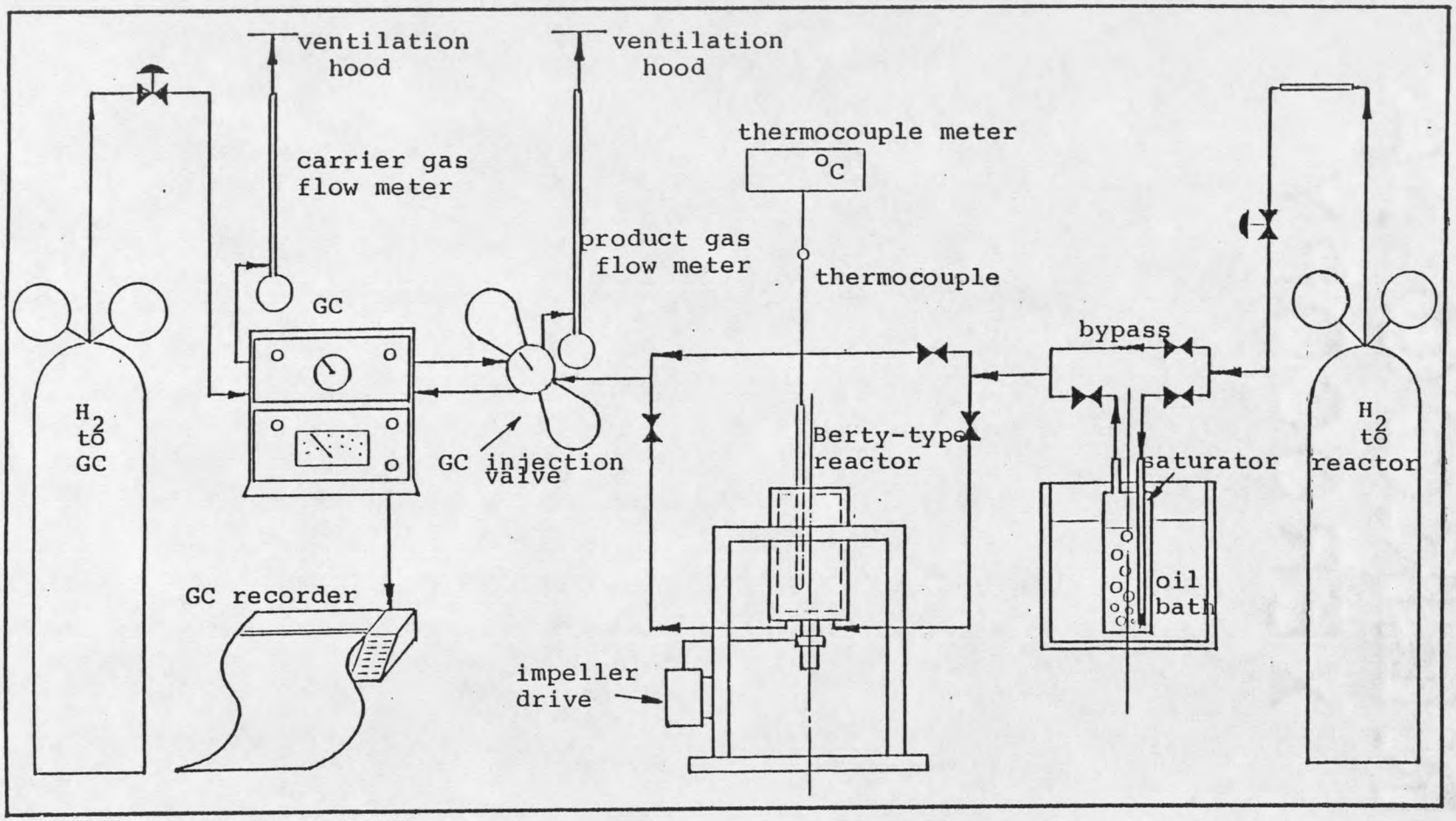

Figure 9. Schematic diagram of experimental apparatus.

saturator, as shown in Fig. 10. The metal saturator replaced a previous glass saturator because metal has better properties for heat transfer than glass. Also the metal saturator can stand high pressure conditions. A parafin oil bath surrounding the saturator was used to control the saturation temperature. P-cymene partial pressure in H_2 flow can be calculated based on the saturation temperature.

Reactor

The cracking reaction was carried out in the continuous flow reactor (Berty-type reactor) with a fixed-catalyst bed, as shown in Fig. 11. An impeller inside of the reactor highly circulated (RPM=1500) the gas during the cracking reaction. In this way p-cymene can be well circulated internally contacting solid catalyst and maintaining constant concentration. The reactor temperature was controlled by external electrical heaters. A K-type thermocouple was located inside of the reactor to measure the reaction temperature. This reactor was the same as used in the o-xylene isomerization study.

Analytical System

The product mixture was sampled by using a 1/8" eight-port valve. Sampling loops are used to inject 1.48 ml of product gas into the gas chromatograph. A soap-film flowmeter was placed after the sample loops to measure the product mixture flowrate, which was required for p-cymene conversion calculation.

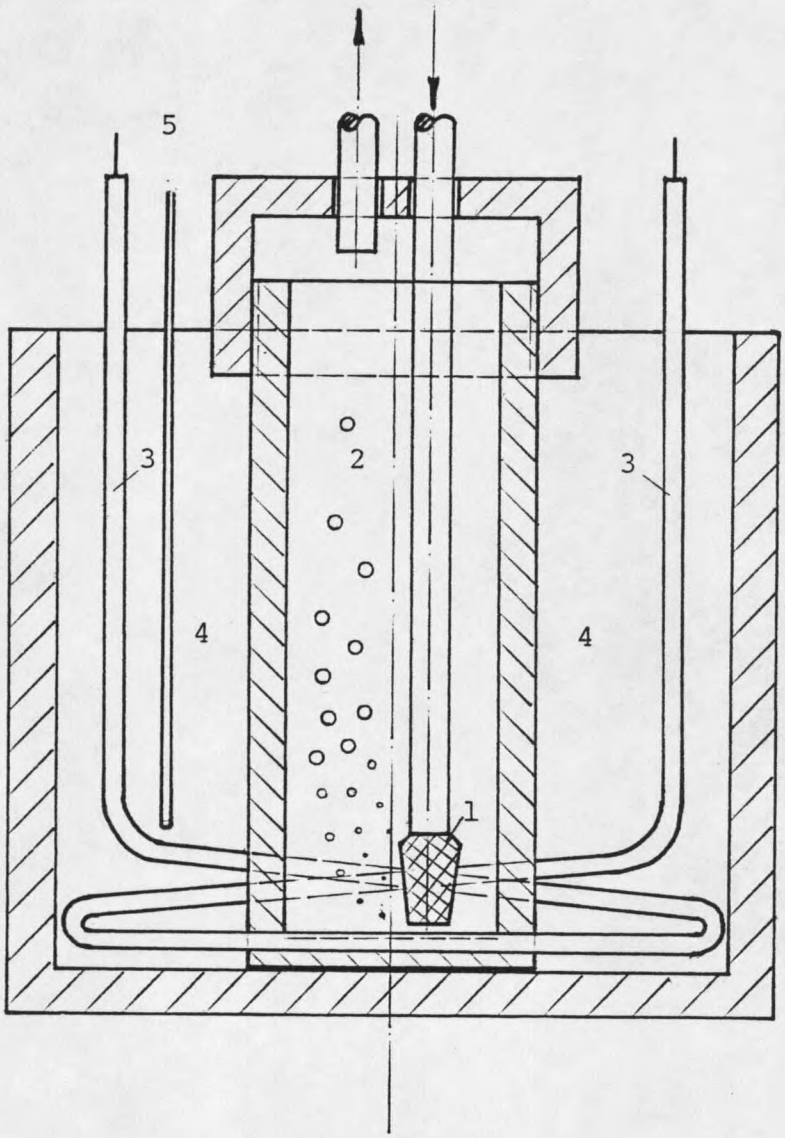

Figure 10. Schematic diagram of the saturator. 1. dispersion tube. 2. liquid p-cymene. 3. electrical heater. 4. parafin oil bath. 5. thermometer.

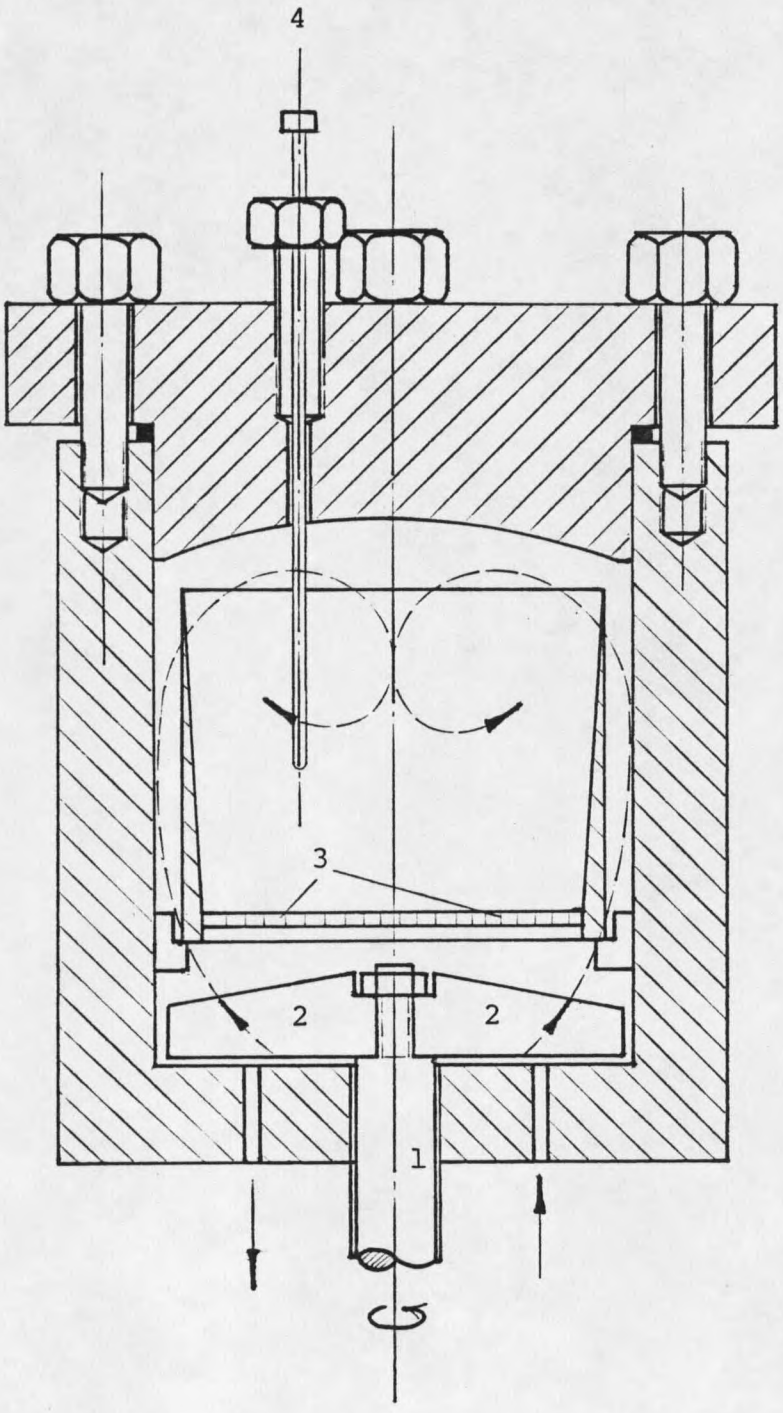

Figure 11. Schematic diagram of Berty reactor. 1. magnetic drive. 2. impeller. 3. catalyst bed. 4. thermocouple.

A gas chromatograph separated the product gases by their different adsorption behavior and quantified the unreacted p-cymene left after cracking. The GC used was fitted with a low volume thermal conductivity detector. Dry hydrogen was supplied to the GC as a carrier gas. A soap-film flowmeter was fixed at the exit of GC to measure the carrier gas hydrogen flowrate. The carrier gas flow rate was kept at the same value throughout the experimental program.

Heating System

The delivery lines and fittings in the whole system are wrapped by heating tapes to prevent p-cymene condensation. The temperatures of lines and fittings need to be much higher than that of saturator because any small cooling point will cause p-cymene condensation. Usually the temperature of p-cymene vapor from saturator is about 93 - 100^0C, so the temperatures for lines and fittings were as high as 110 -140^0C.

Experimental Procedures

There were two experiments for each reaction run:

1. The blank experiment to determine p-cymene mass flow rate into the reactor at an operating condition.

2. The reaction experiment to measure the p-cymene conversion at an operating condition.

Blank Experiment

The system for blank measurements was operated without a

catalyst in the reactor. Two kinds of data can be determined by blank measurements: (1) p-cymene mass flow rate as it changed with saturator temperature, p-cymene liquid level in the saturator, and H_2 flow rate through the saturator, (Those parameters were a little different in each experimental run. With blank measurements, the mass flow rate of cymene can be given by GC recorder.) and (2) the reactant purity. (With GC analysis, the mean composition of reactant feed to reactor was 98% of p-cymene and 2% of cumene at a temperature of 93.3^0C.)

Experimental Method. The reactor was heated to the expected temperature and then hydrogen was allowed through the saturator to vaporize p-cymene. Once p-cymene entered into the reactor, the impeller was set at 1500 rpm for internal circulation. The exit of reactant was then checked by GC recorder every 10 minutes. Each blank experiment ran for 60 minutes.

Reaction Experiment

The system for p-cymene cracking reaction was operated with catalysts in the reactor at expected reaction conditions. The p-cymene conversion was then determined in this experiment.

Experimental Method. The test cata[Bst pellets were weighed into the basket (about 0.1 g). The basket was set into the reactor, which was then assembled. Hydrogen was directed through the bypass into the reactor to sweep off

air in the reactor. When the reactor was heated up to the desired temperature, hydrogen was directed through the saturator to deliver p-cymene vapor to the reactor. Meanwhile the impeller was set to 1500 rpm. Samples of product gas were injected into the GC every 10 minutes. Temperatures of the reactor, saturator, and GC as well as hydrogen flow rate were adjusted to be the same as much as possible. Each reaction ran for 100 minutes at the set conditions.

Calculations

P-cymene Mass Flow Rate

In blank experiment, GC recorder gave the integrated peak area which indicated the amount of p-cymene into the reactor at the performing conditions.

P-cymene mass flow rate was calculated as follows:

$$m = (G \times A_O \times f)/v_O$$

where

m = mass flow rate of p-cymene into the reactor (g/sec)

G = calculation constant (g-cymene/unit area)

A_O= GC peak area of input p-cymene (area unit)

f = p-cymene flow rate from the sample loop (ml/sec)

v_O= sample loop volume (ml)

The calculation constant k was determined at different temperatures and hydrogen flow rates. When the temperature of GC was about 122.5^{0}C and the carrier gas (H_2) flow rate was about 16 ml/min, the G was determined as 1.94×10^{-9} g-cymene/unit area. Sample loop volume was 1.48 ml.

P-cymene Conversion

The p-cymene conversion was determined by using the integrated GC peak areas as recorded by the HP 3380A. The conversion was calculated from the area fraction of the unreacted p-cymene to the input of p-cymene during the reaction at the same temperature as blank experiment.

The p-cymene conversion was calculated as follows:

$$X = (1 - A/A_O) \times 100\%$$

where

X = p-cymene conversion in cracking reaction (%)

A = GC peak area of unreacted p-cymene (area unit)

A_O= GC peak area of input p-cymene (area unit)

Reaction Rate

The Berty-reactor operating at a high recycle ratio yields the appearance of mixed flow reactor behavior. For the reactant well mixed with the catalysts inside of the reactor, the reaction rate was calculated as follows:

$$-r = (m \times X)/(W \times S \times M)$$

where

$-r$ = the rate of disappearance of p-cymene in cracking reaction (moles p-cymene/$m^2 \cdot sec$)

m = mass flow rate of p-cymene (g/sec)

X = p-cymene conversion in cracking reaction (%)

W = mass of test catalyst (g)

S = surface area of test catalyst (m^2/g)

M = molecular weight of p-cymene (134 g/mole)

Rate Constant

With the assumption of first order reaction for p-cymene cracking (in similarity to xylene isomerization [28,29]):

$$-r = k \times C_{cymene}$$

where

$-r$ = reaction rate of p-cymene cracking (moles/$m^2 \cdot s$)

k = rate constant of p-cymene cracking (1/sec)

C_{cymene}= surface concentration of p-cymene on the test catalysts (moles-cymene/m^2)

(Note: No definite order has been determined for p-cymene cracking. The mechanism will be discussed later in this thesis.)

The rate constant k can then be calculated based on a continuous Berty type reactor:

$$k = \frac{m}{M}\left[\frac{X}{1 - X}\right]$$

where

k = reaction rate constant (1/second)

m = p-cymene mass flow rate (g-cymene/sec)

M = weight of the test catalyst (gram)

X = p-cymene conversion during the reaction

Problems In The Experiment

The loops and fittings in the apparatus must have a temperature over 120 ^{0}C because p-cymene saturation is at a temperature of 200 ^{0}F(93.3 ^{0}C) throughout this system. It is easily condensed at nominal temperatures less than 100 ^{0}C because of local cooling points.

The operation parameters such as carrier gas flow rate, GC oven temperature, dry H_2 flow rate and saturator temperature must be maintained as constant as possible. In this way the experimental data is dependable and believable.

In p-cymene cracking reaction, C_2H_4 and C_2H_6 are products with molecular weight 28 and 30 respectively. Air has a very similar molecular weight (28.84). Before the reaction runs, all the air should be completely purged off to avoid an air leak which might be interpeted as C_2H_4 and C_2H_6 peaks.

RESULTS AND DISCUSSIONS

System Parameters

Catalysts with 2.8%, 6.1%, 8.5%, 15.0%, 24.5%, 38.7%, and 54.1% Al_2O_3 content were used in measuring cracking activities in this research work. As given in Table 6, cracking reactions were carried out at 220^0C, 250^0C, 290^0C, and 315^0C, respectively.

In preliminary experiments, several experimental parameters were determined.

Saturator temperature was set near 200^0F (93.33^0C) to provide p-cymene vapor into the reactor. The loop average temperature must be 20-40 ^0C above the condensation point to prevent cool spot condensation, thus the available heating equipment heated the system loops and fittings up to $120-140^0C$. If the temperature of saturator is too high, a serious condensation problem will happen in the system.

The Gas Chromatograph oven temperature was set at about 125^0C. The temperature must be higher than that in the saturator ($>100^0C$), because p-cymene vapor will condense in the GC if the oven temperature is lower than 100^0C. The temperature upper limit for this GC column is 150^0C, so the oven temperature cannot be allowed higher than 150^0C.

Several carrier gas (H_2) flow rates had been tried in the preliminary experiments, and the flow rate between 15 to 20 ml/min showed the best graphical results from the GC recorder for this experiment.

The operating parameters are listed in Table 6.

Table 6. Experimental Parameters.

parameters in saturator		
oil bath temperature (^0C)	H_2 pressure (psi)	p-cymene vapor pressure (psi)
93	40	∿0.99

parameters in reactor			
reaction temperature (^0C)	product flow rate (ml/min)	sample	impeller speed (RPM)
220	41	A-10, A-44, A-65	1500
250	41	A-10, A-44	1500
290	41	A-10, A-44	1500
315	41	A-3, A-7, A-10 A-18,A-26,A-44,A-65	1500

parameters in Gas Chromatograph		
GC temperature (^0C)	carrier gas H_2 flow rate (ml/min)	detector current (mA)
∿122	16	150

Catalytic Activity For P-cymene Cracking

To examine catalytic activity as a function of alumina-content, a series of experiments with silica-aluminas of different alumina content were performed in p-cymene

cracking reaction at 315^{0}C. Different initial activity values were obtained from different catalysts and all of the catalysts (except A-65) were active for the cracking reaction. The experimental data and basic calculations are located in the Appendix.

The hydrocarbon product distribution which includes molecules from 2 carbon atoms up to 10 carbon atoms, is shown in Table 7 for all samples. Three peaks appeared in GC recorder for p-cymene cracking. At the GC operating conditions (Table 6), the first peak has the same retention time as C_2H_6-C_3H_8; the second peak has the same retention time as toluene; the third peak is related to unreacted p-cymene in the reactor. The peak appearances for xylene and cumene were not found at temperature of 220 to 320^{0}C for all samples. In Table 7, C_3- refers to C_1, C_2, C_3 fraction hydrocarbons.

Table 7. Product Distribution of P-cymene Cracking*.

Reaction temperature: 315^{0}C				
sample	first peak C_3- frac. (%)	second peak toluene (%)	third peak unreacted cymene (%)	p-cymene conversion (%)
A-3	ND	36	60	40
A-7	ND	36	58	42
A-10	ND	39	54	46
A-18	ND	31	67	33
A-26	ND	34	60	40
A-44	ND	31	65	35
A-65	0	0	100	0

* The value indicate the mole percentage.
ND Not detectable for C_3 alone.

The first peak is a mixture of CH_4, C_2H_6, and C_3H_8 light hydrocarbons and some air leak may contaminate the peak area, so the quantity of this peak cannot be determined. However, blank runs have never shown strong air leakage under controlled conditions. Theoretically, toluene should have the same number of moles as that of reacted p-cymene, but there is a small difference between these two values for all samples. This can be explained as coke formation: since coke is formed during cracking reaction, some C_7 fraction hydrocarbons participate in the coke formation and turn to carbonaceous materials as they cover the catalyst surfaces.

A relationship between alumina content and cracking activity is found in following figures. Fig. 12 plots the catalyst-surface-area specific reaction rate against alumina content, and Fig. 13 presents the conversion of p-cymene cracking as a function of alumina content.

Sample A-0 is found at the origin in Fig. 12-13 because no cracking reaction could be measured on pure silica gel. The reason is due to no acidity observed on silica gel. This is also reported in the literature [1,18].

In Fig. 12, cracking reaction rates are evident at low values of alumina-content catalyst, become larger at high alumina contents, and then fall to zero for very large alumina-content catalysts because high Al-content samples have very low surface areas and acidities (samples of 54% and 88% Al_2O_3 are shown in Table 5). Both Fig. 12 and Fig.

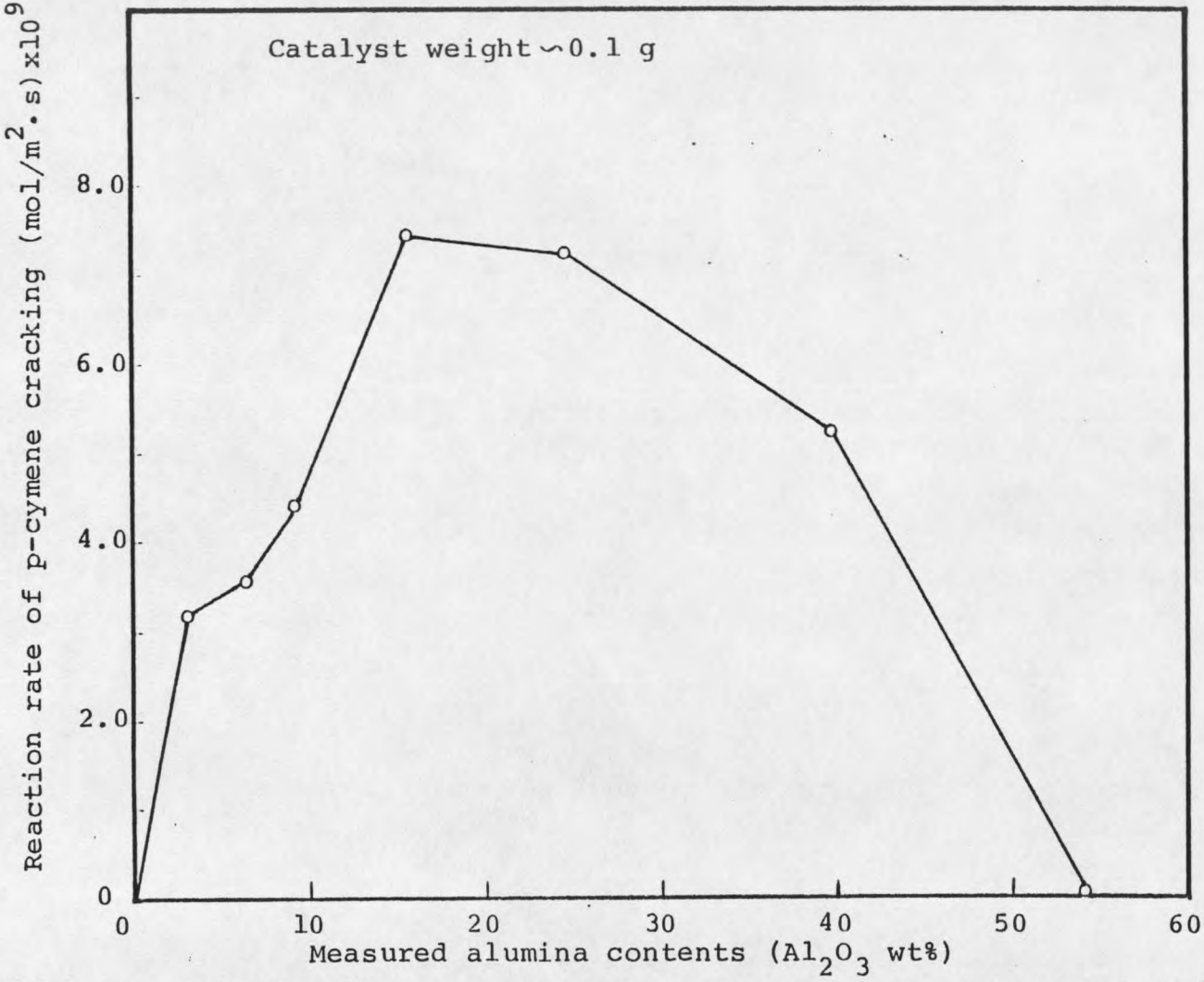

Figure 12. Ralationship of reaction rate for p-cymene cracking at 315°C to the measured alumina contents in the catalysts.

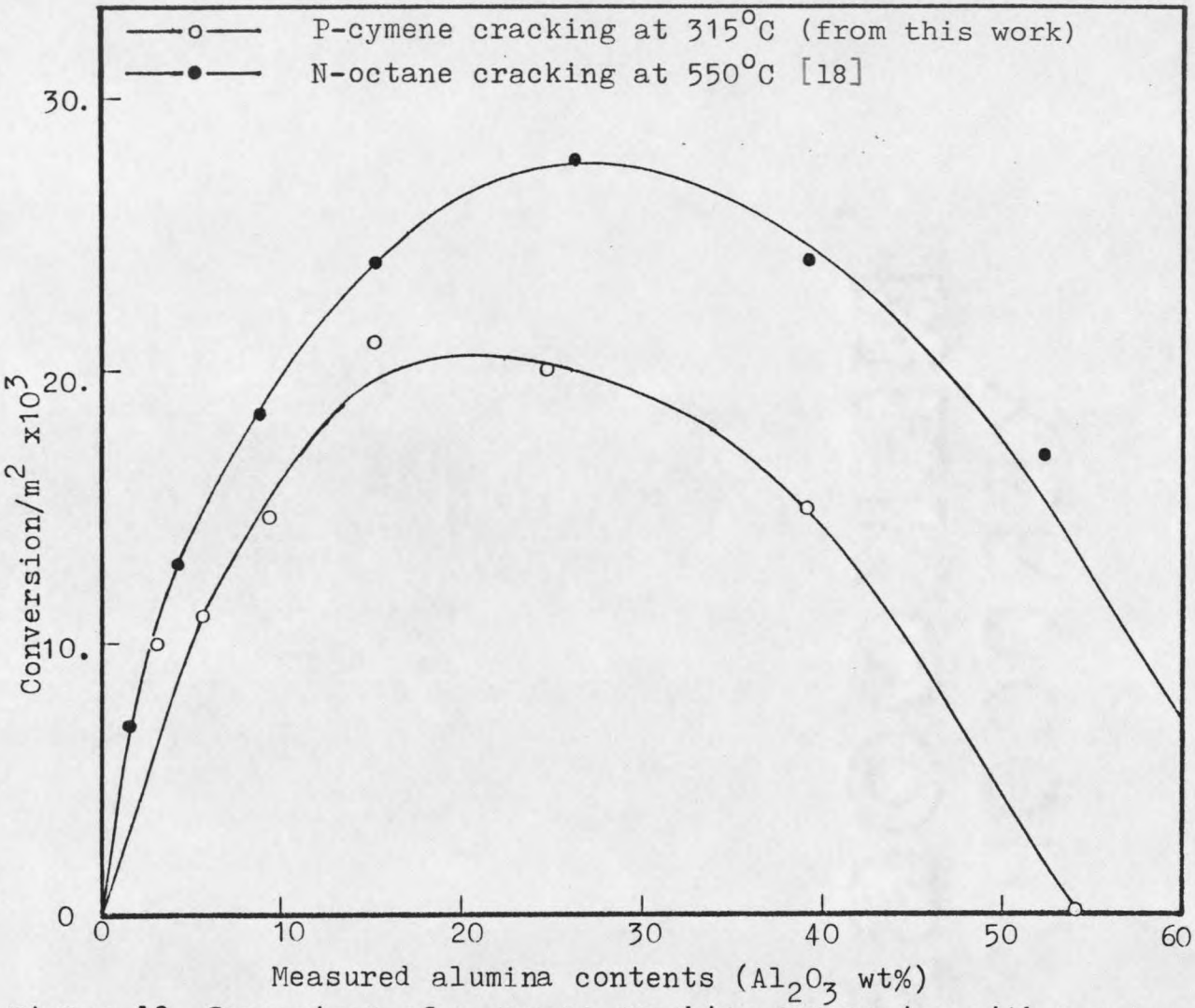

Figure 13. Comparison of p-cymene cracking conversion with n-octane cracking conversion.

13 indicate that the highest activity for p-cymene cracking is at 15-25% Al_2O_3 in the silica-aluminas. For comparison of cracking reactions, the activity of n-octane cracking reaction as observed by Holm and Clark [18] over silica-aluminas is also given in Fig. 13. In their work, the n-octane cracking activity was related to the apparent alumina content and here the activity is corrected to relate the measured alumina content. The conversion of apparent and measured alumina content in catalysts is located in the Appendix. The high activity range for n-octane cracking appears at about 20-30% Al_2O_3. Both p-cymene cracking and n-octane cracking curves show the same pattern.

Effect of Acidity On Catalytic Activity

One of the objectives of the present work is to find the relationship between cracking activity and acidity of the silica-alumina materials synthesized. J. Golden quantified the strong acid sites on the test catalysts by using CAEDMON energy distribution calculations [9]. This information is given in Fig. 3 (in Literature Survey) with strong acid content per surface area as a function of bulk alumina content. J.A. Schwarz determined the number of Lewis acid sites, Bronsted acid sites, and total acid sites by using the infrared spectrum of pyridine adsorption along with a standard titration technique [14]. The information has been listed in Table 2 in this thesis. For the purpose of

uniformity and comparison, the acidities per surface area as a function of bulk alumina content are calculated and given in Fig. 14. Comparing Fig. 3 and 14, they show different patterns of acidity for silica-aluminas. This is because Fig. 3 represents strong acid site acidities only, whereas Fig. 14 gives the total acidity which includes both weak and strong acid strengths.

Effect of Total Acidity

Fig. 15 plots the surface-area-specific reaction rates for p-cymene cracking reaction against the strong acid site strength which was observed by Golden. The reaction rates from all samples except A-18 follow a increasing curve with increased strong acidity. At a range of low alumina content catalysts, the activity of p-cymene cracking is going up with increasing acidity, rising sharply at an acidity of 0.6-0.7 $\mu eq/m^2$. It can be observed that the p-cymene cracking activity is positively affected by strong acidity in a low alumina range. But a direct relationship between cracking activity and catalyst acidity has not been found in this figure.

A relationship between cracking activity and total acidity of silica-aluminas is shown in Fig. 16 in which the acidities of catalysts were determined by J.A. Schwarz. The same kind of relationship as obtained by Golden is also found in this figure. The cracking activity start at low

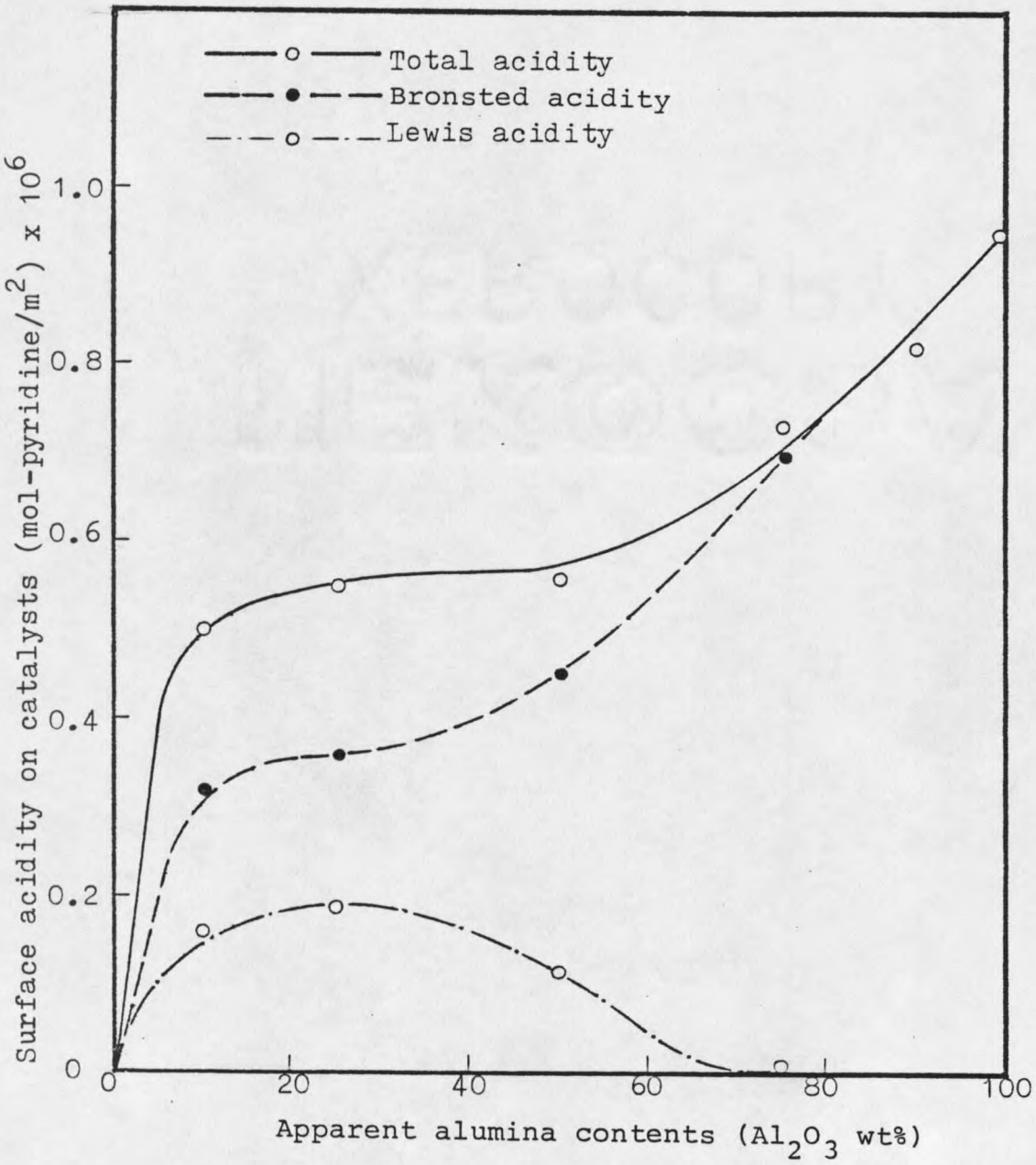

Figure 14. Total acidity, Lewis acidity, and Bronsted acidity as a function of apparent alumina contents [14].

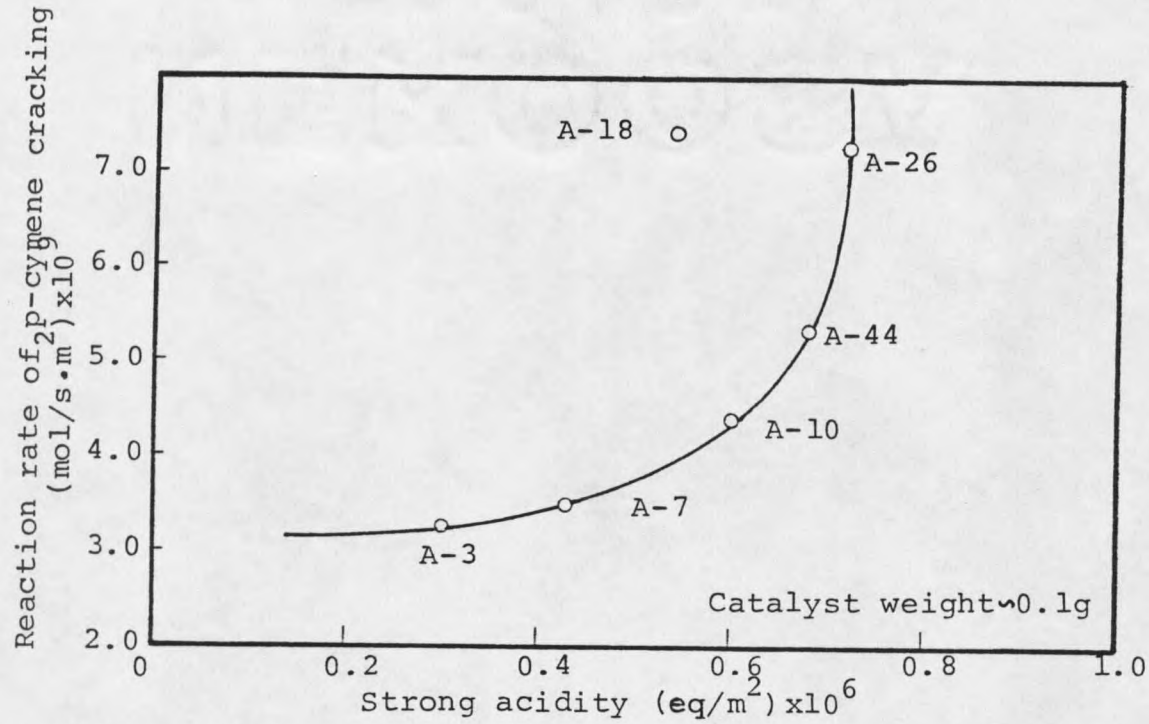

Figure 15. Catalytic activity of p-cymene cracking as a function of strong acidity (from Golden).

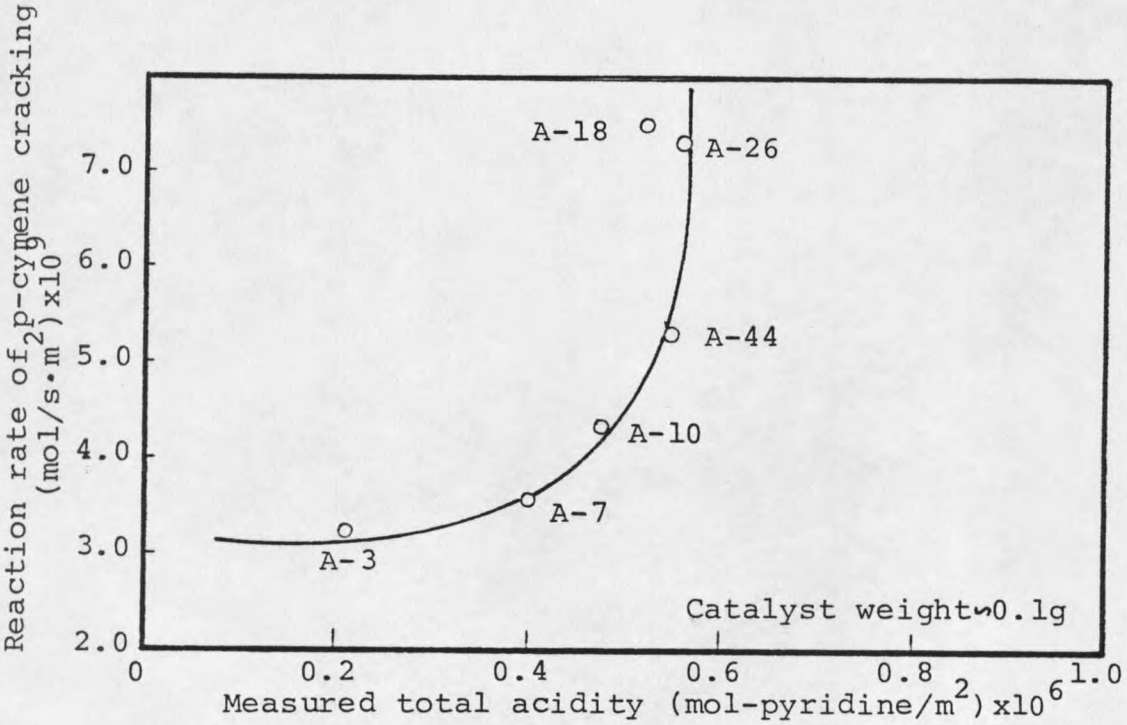

Figure 16. Catalytic activity of p-cymene cracking as a function of total acidity (from Schwarz).

acidity and sharply increases at an acidity of 0.55 μmole-pyridine/m^2. The curves in Fig. 15 and 16 are generally in good agreement. It is reasonable to infer that either strong acidity or total acidity provides some activity to p-cymene cracking. This result is consistent with the work of U.A. Sedran et al. where they correlated the activity of methanol transformation into hydrocarbons and the acidity of silica-aluminas and concluded that the activity increases with the increments of acidity in the low total acidity range [27].

An anomaly for sample A-18 is observed in Fig. 15 in that the catalytic activity of A-18 is off the curve. This can be explained as an experimental error. The catalyst preparation may cause some differences in catalyst surface areas. Conversely, even under the same preparation condition, same procedure, and same PH control, factors such as calcination temperature, time period, catalyst position in the oven, and air flux in the oven will cause surface area differences. For sample A-18, the surface area is much lower than others, indicating a possible sintering effect, and hence much lower acidity.

Effect of Bronsted Acidity

To determine Bronsted acidity on a series of silica-aluminas which were used in p-cymene cracking reaction, a correction method was used for this purpose. The correction was introduced by J.Golden in his thesis, where he correlated a relation between o-xylene isomerization and

Bronsted acidity [9]. The idea for Bronsted acidity correction is that the total acidity of catalysts is the summation of Lewis acidity and Bronsted acidity. Lewis acidity can be considered as the acidity associated with pure alumina. In this way, the acidity associated with pure alumina is subtracted from the measured acidity for each sample on a weight fraction basis, then the corrected Bronsted acidity for all samples are obtained in Table 8.

Table 8. Corrected Bronsted Acidity [9].

sample	total acidity ($\mu eq/m^2$)	Bronsted acidity ($\mu eq/m^2$)
A-3	0.285	0.272
A-7	0.430	0.402
A-10	0.593	0.554
A-18	0.544	0.475
A-26	0.709	0.597
A-44	0.696	0.519
A-65	-	-
A-88	0	0
A-100	0.442	0

Fig. 17 presents the surface-area-specific reaction rate for p-cymene cracking as a function of Bronsted acidities which are the corrected values in Table 8. The cracking activities are basically following a straight line with changes of Bronsted acidity. This linear relationship

between cracking activity and Bronsted acidity suggests that Bronsted acid sites are active sites and directly participate in the cracking reaction. This can be explained as follows: since carbonium ion formation is a major step in cracking reactions, which has been shown in the literature [1], the Bronsted acid site can provide protons to p-cymene molecules and an intermediate product, a carbonium ion, will be formed on the Bronsted acid sites. Subsquently there is a cracking of carbonium ions and formation of products. In this way, Bronsted acid sites exhibits catalytic activity.

Fig. 18 plots the same reaction rate against assumed Bronsted acidity, which was determined by Schwarz's spectrum of pyridine adsorption and assumption of similar catalyst morphology. In this figure all the samples fit a straight line along with Bronsted acidity. Both Fig. 17 and 18 give the linear correlation between cracking activity and Bronsted acidity. Fig. 18 further explains that Bronsted acidity contributes active sites to cracking reaction and directly affects cracking activity, such as p-cymene cracking.

Effect of Lewis Acidity

To determine the relationship between catalytic activity and Lewis acidity, the surface-area-specific reaction rate for p-cymene cracking is plotted against the Lewis acidity distribution which was obtained by J.A. Schwarz in Fig. 19. The same assumption of similar catalyst morphology was used.

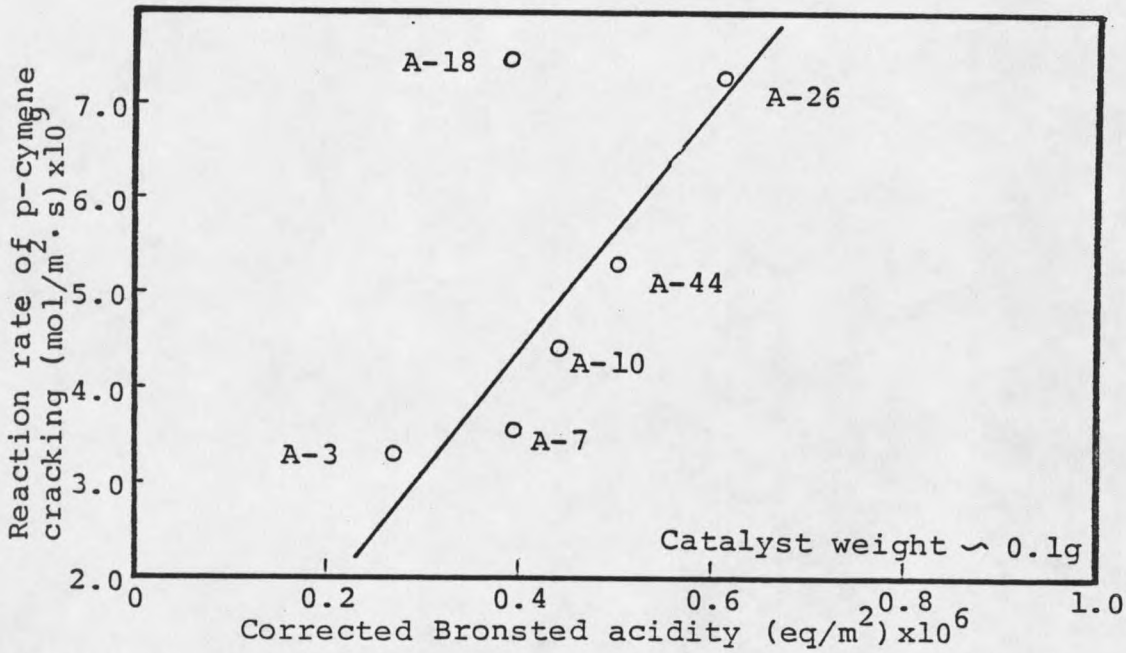

Figure 17. Catalytic activity of p-cymene cracking as a function of corrected Bronsted acidity (from J. Golden).

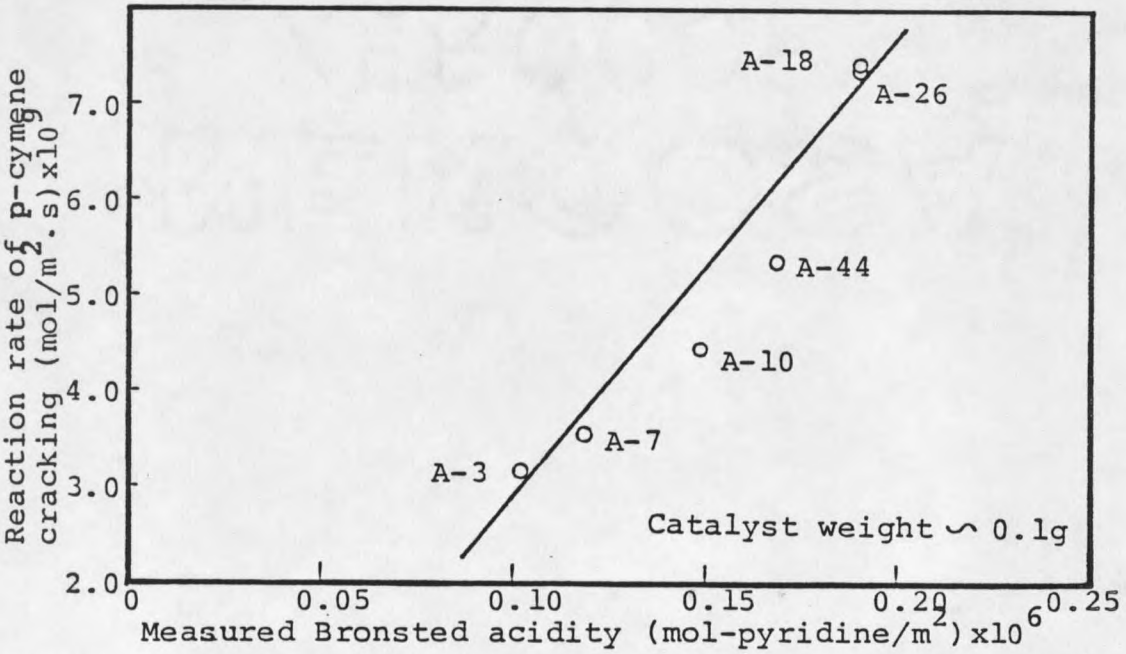

Figure 18. Catalytic activity of p-cymene cracking as a function of measured Bronsted acidity (from J.A. Schwarz).

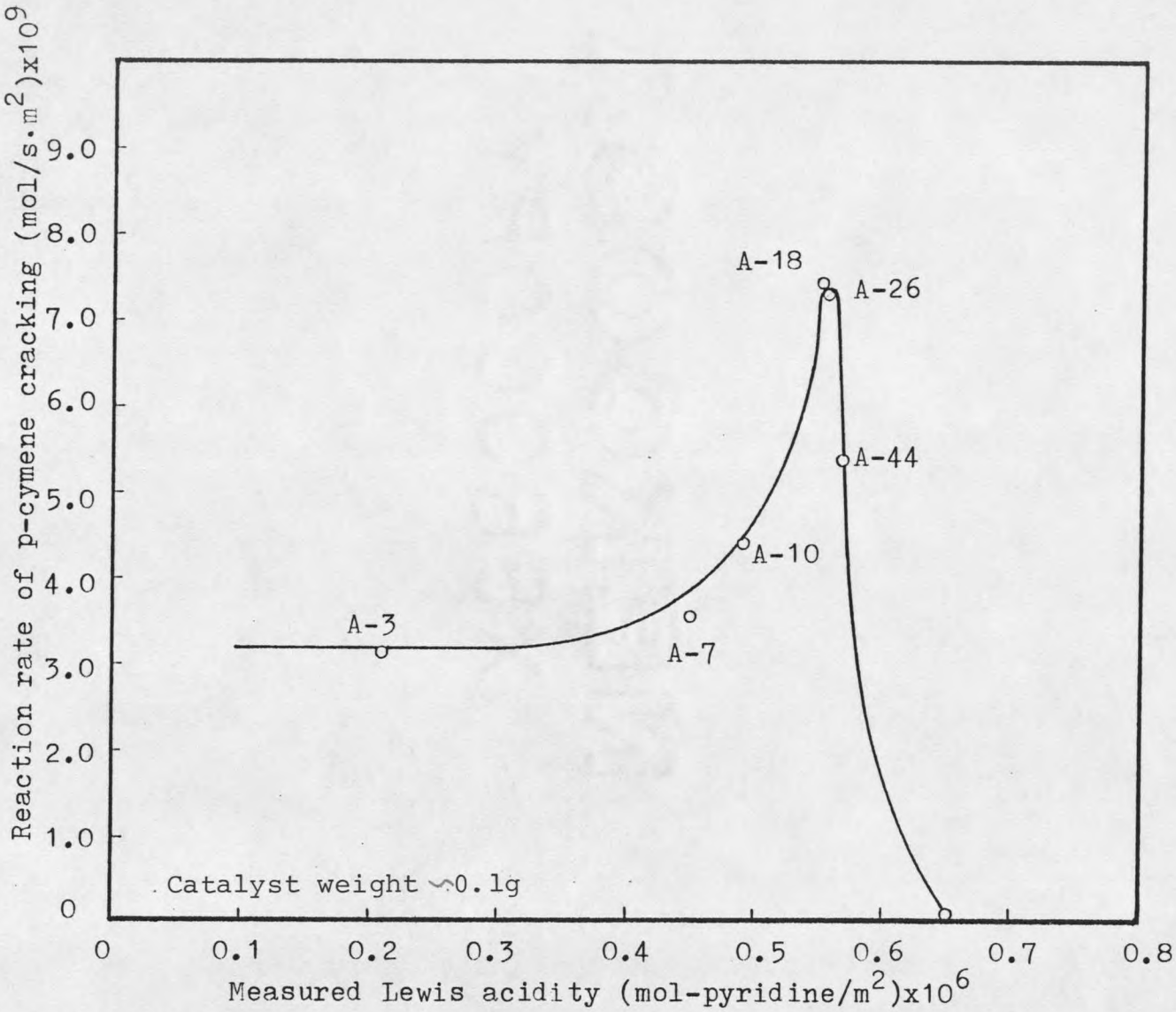

Figure 19. Catalytic activity of p-cymene cracking as a function of measured Lewis acidity (from J.A. Schwarz).

In Fig. 19, there is not a direct relationship between reaction rate of p-cymene cracking and Lewis acidity. It is clear that the function of Lewis acidity is different from that of Bronsted acidity.

In general, Lewis acidity seems not to determine cracking activity, as shown in Fig. 19. However, Lewis acid sites are possibly operating indirectly by enhancing the acidity of adjacent Bronsted sites through charge withdrawal from the O-H bond. Cracking activity decreases very rapidly at high Lewis acidity. This character might be due to the fact that Lewis acidity is too active for hydrocarbon cracking, thus coke formation occurs on the catalyst surfaces. The carbonaceous materials cover the acid sites and mask the catalytic activity.

Another way to correlate catalytic activity and acidity distribution on the catalysts is shown in Fig. 20 and Fig. 21. Fig. 20 presents the activity of p-cymene cracking, total strong acidity as determined by J. Golden, and corrective Bronsted acidity as a function of Al_2O_3 contents. As can be seen, there is an excellent consistency between catalytic activity and the Bronsted acidity. The cracking activity curve follows the same pattern as total strong acidity at low alumina-content range, but is quite different at high alumina-content range. Fig. 21 shows the same cracking activity comparing with the total acidity and Bronsted acidity as determined by modified titration figure

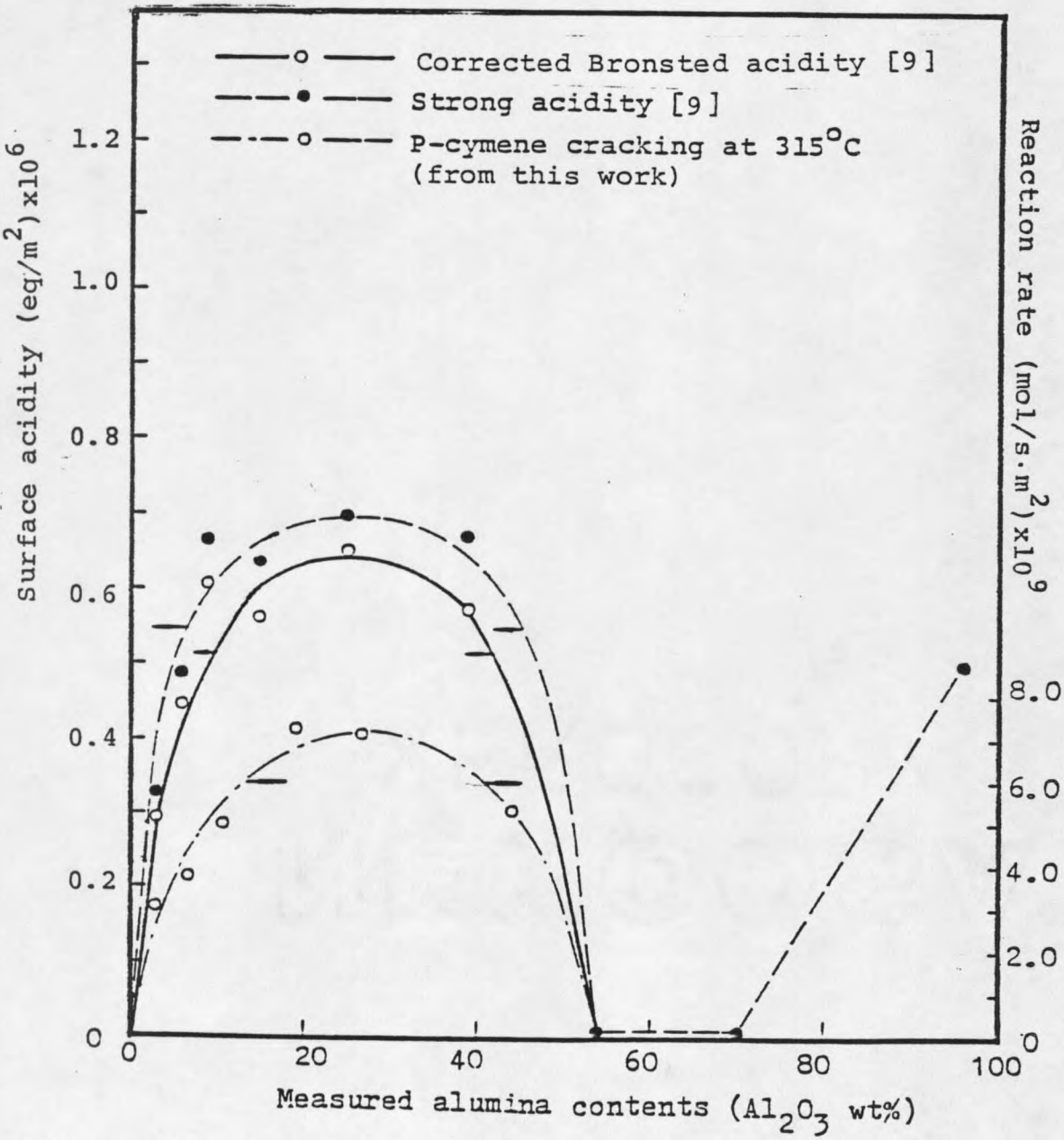

Figure 20. Relationships of activity and acidity to the measured alumina contents in catalysts.

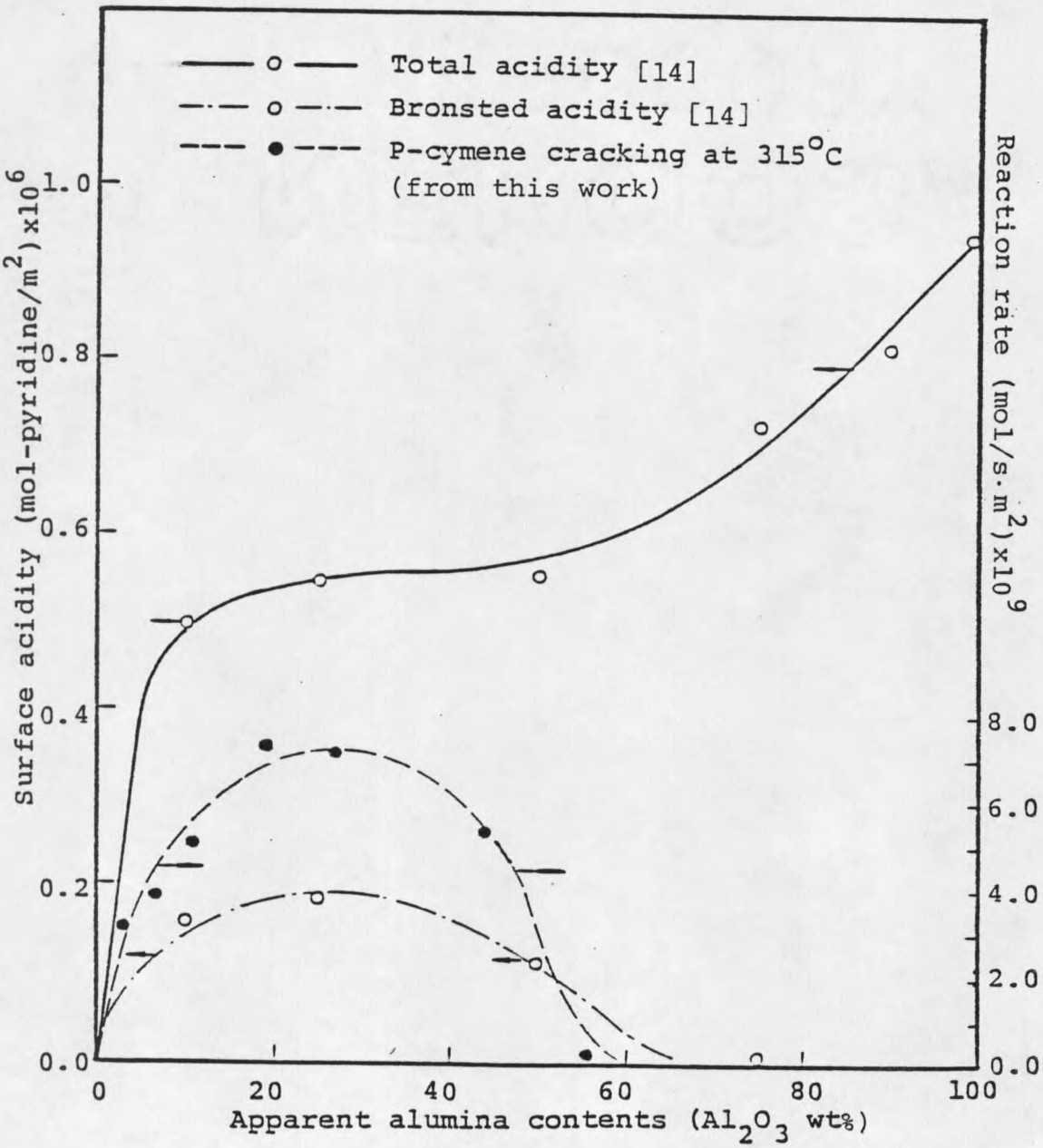

Figure 21. Relationships of activity and acidity to the apparent alumina contents in catalysts.

technique from J.A. Schwarz using the previously cited assumptions. The same pattern is obtained in Fig. 21 in that the cracking activity is in good agreement with Bronsted acidity and with total acidity at low alumina-content range. It is clear that the Bronsted acid site plays an important role in cracking reaction, as discussed before. Here the p-cymene cracking activity is corrected to relate apparent alumina content by using the conversion method which is located in the Appendix.

Comparison of Cracking and Isomerization

Catalytic Activity Comparison

The test catalysts used in the p-cymene cracking reaction are the same series of silica-aluminas in previous o-xylene isomerization. A comparison for conversion of p-cymene cracking and conversion of o-xylene isomerization which was obtained by J. Golden is given in Fig. 22. The p-cymene cracking reaction took place at 315^0C and the o-xylene isomerization was at 300^0C. As can be seen, the conversion for p-cymene cracking is consistent with the conversion for isomerization. The consistency of these two curves exhibits that silica-alumina materials apparently have the same contribution to both cracking reaction and isomerization. The same results are also observed in Holm and Clark's work in Fig. 4 (in Literature Survey) where cracking reaction of n-octane and isomerization of o-xylene

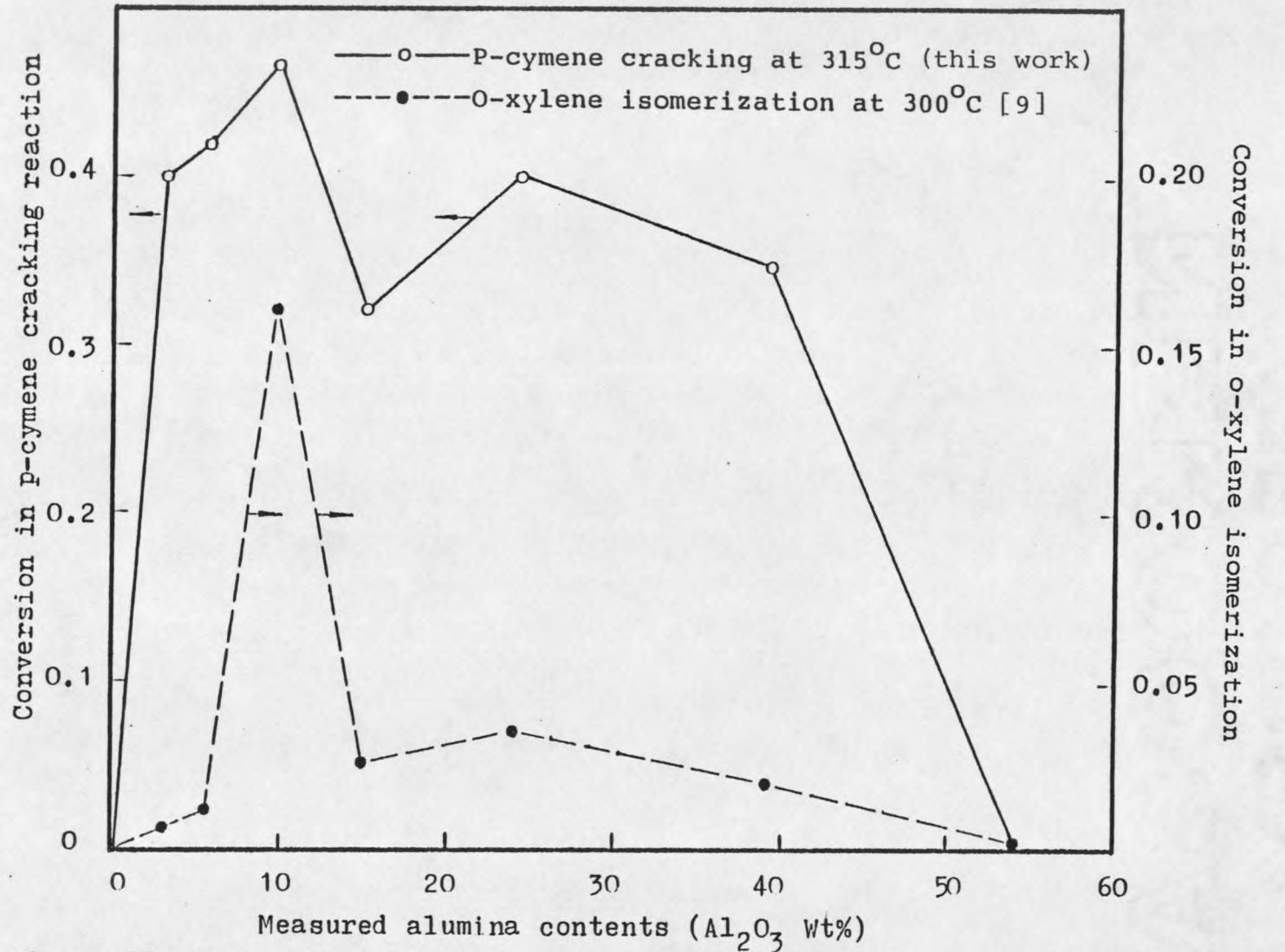

Figure 22. Conversions of p-cymene cracking and o-xylene isomerization as a function of alumina contents.

show the same activity pattern over silica-alumina catalysts [18].

For a further correlation of cracking reaction and isomerization, the rate constants were calculated and compared in Fig. 23 and 24. The rate constant, k, for p-cymene cracking and o-xylene isomerization were calculated by using the equation of first-order reaction. O-xylene isomerization has been proved as first-order reaction [28,29] and p-cymene cracking was assumed as first order reaction.

The rate constants of p-cymene cracking were calculated at a temperature of 315^0C. The reaction for o-xylene isomerization were carried out at temperatures of 300-400^0C and their rate constants were converted to 315^0C by using Arrhenius factors.

In Fig. 23 the rate constants for both o-xylene isomerization and p-cymene cracking reactions show the same pattern against alumina content. It suggests that the rate constants are related to alumina content in the catalysts. Furthermore the good compatibility of these two rate constants suggests that cracking reaction and isomerization are the same kind of reactions. Cracking reactions catalyzed by acidic surfaces has been thoroughly studied and carbonium ion intermediates have been shown to form on the catalyst surfaces during the reaction [1]. In isomerization, o-xylene molecules can form a carbonium ion on acidic catalyst

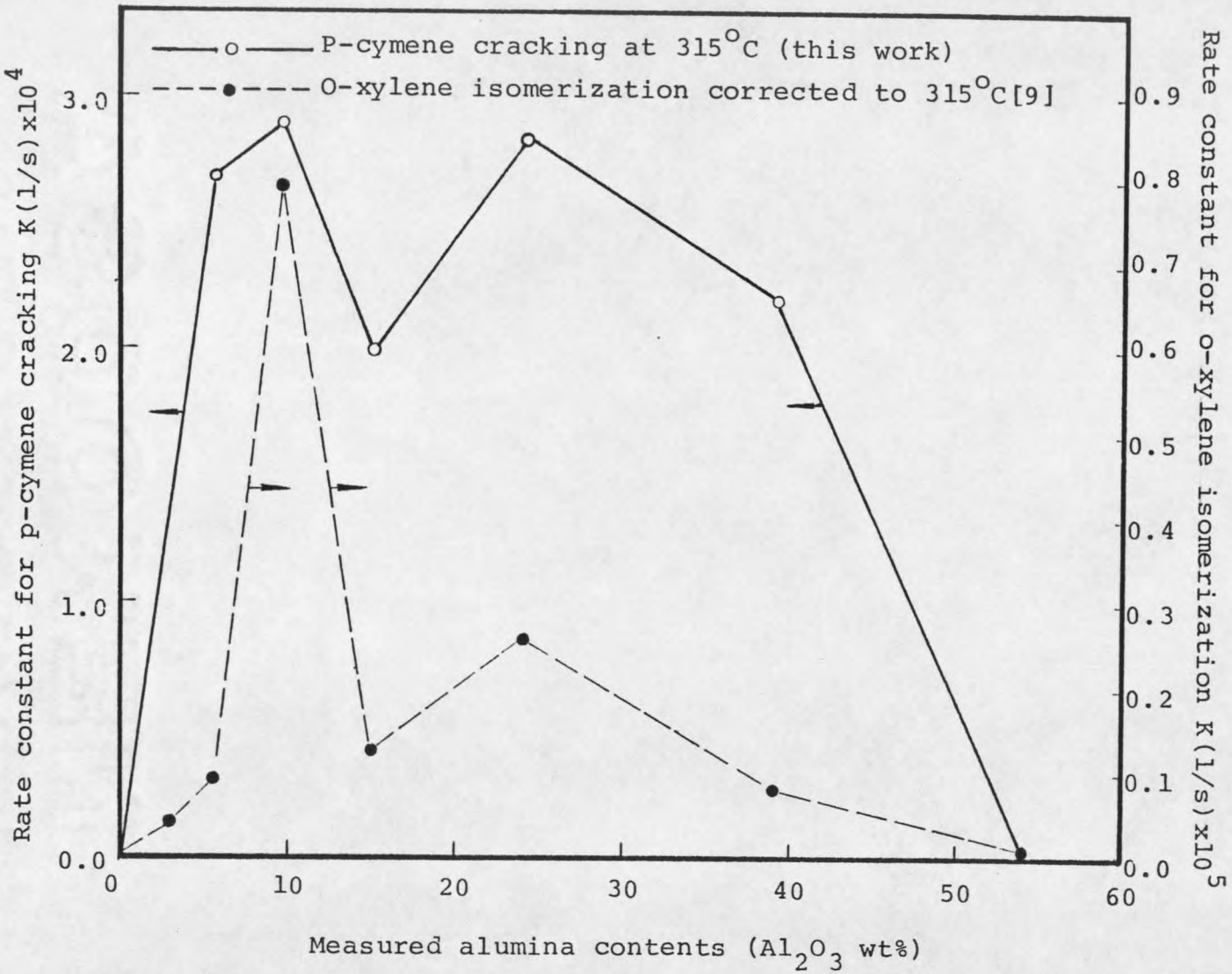

Figure 23. Comparison of rate constants for p-cymene cracking and o-xylene isomerization.

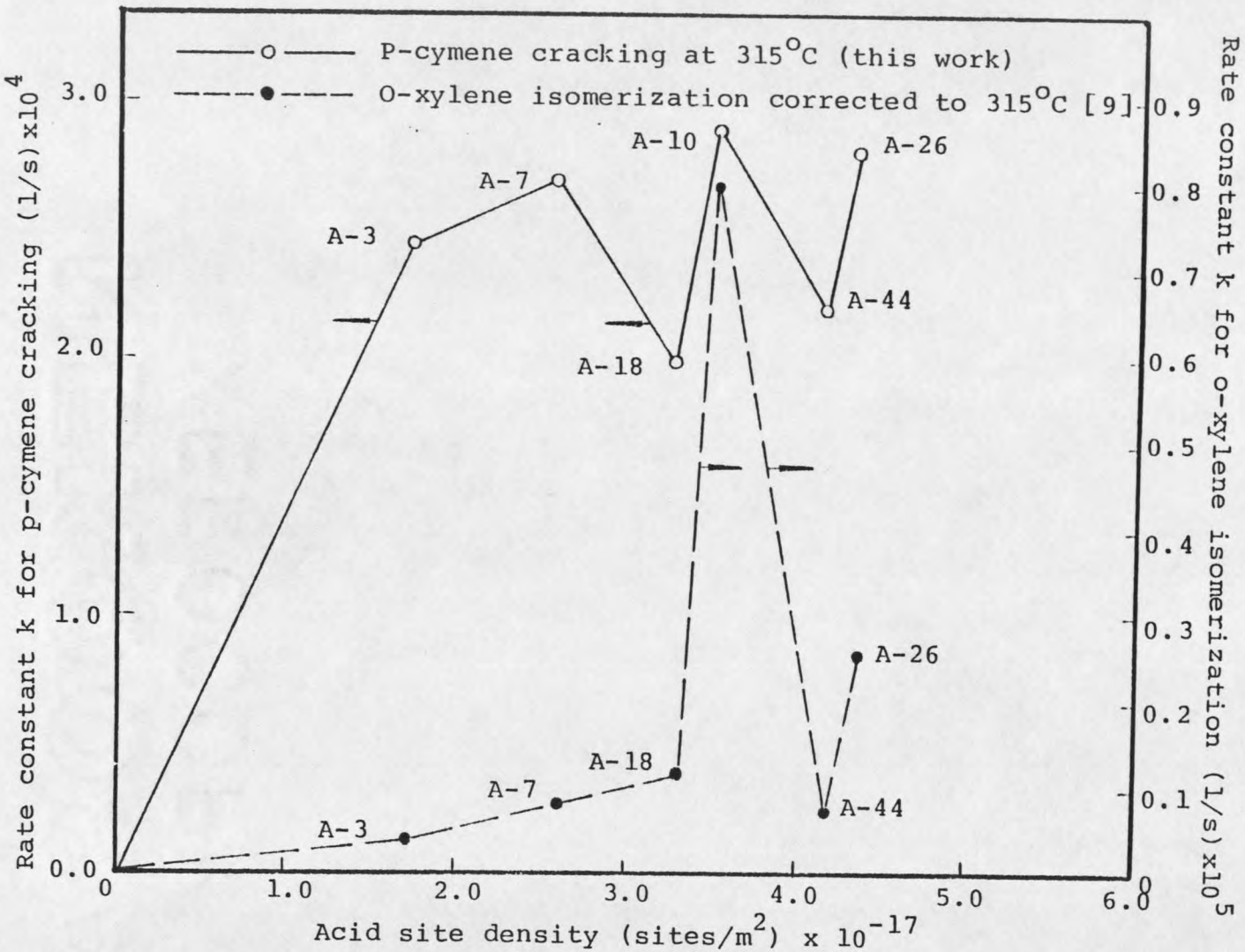

Figure 24. Rate constants of p-cymene cracking and o-xylene isomerization as a function of acid site density (from J. Golden's data).

surfaces and an isomer of xylene (p-xylene) produced.

Fig. 24 shows the rate constants of p-cymene cracking and o-xylene isomerization as a function of acid site density of the test catalysts. As can be seen, the two curves of rate constants are generally following the same pattern. The relationship between rate constants and acid site density exhibits that the high catalytic activities, which are also high values of rate constants, for both p-cymene cracking and o-xylene isomerization appear at the same density range of 3.0×10^{-17} to 4.0×10^{-17} sites/m^2. The consistency of the two reaction rate constants further indicates that p-cymene cracking and o-xylene isomerization are the similar reactions over silica-alumina catalysts.

Activation Energy Comparison

Arrhenius plots have been used to represent the cracking activity of catalysts as a function of temperature. Cracking activity calculations at different temperatures are located in the Appendix. Arrhenius plots based on the rate constants are shown in Fig. 25 and Fig. 26 for samples A-10 and A-44 respectively. Only A-10 and A-44 were used because the purpose for Arrhenius plots is to compare the activation energies of p-cymene cracking with those of o-xylene isomerization and find a relationship between the reactions.

The plots in the Fig. 25 and 26 indicate that samples A-10 and A-44 have essentially the same activation energies

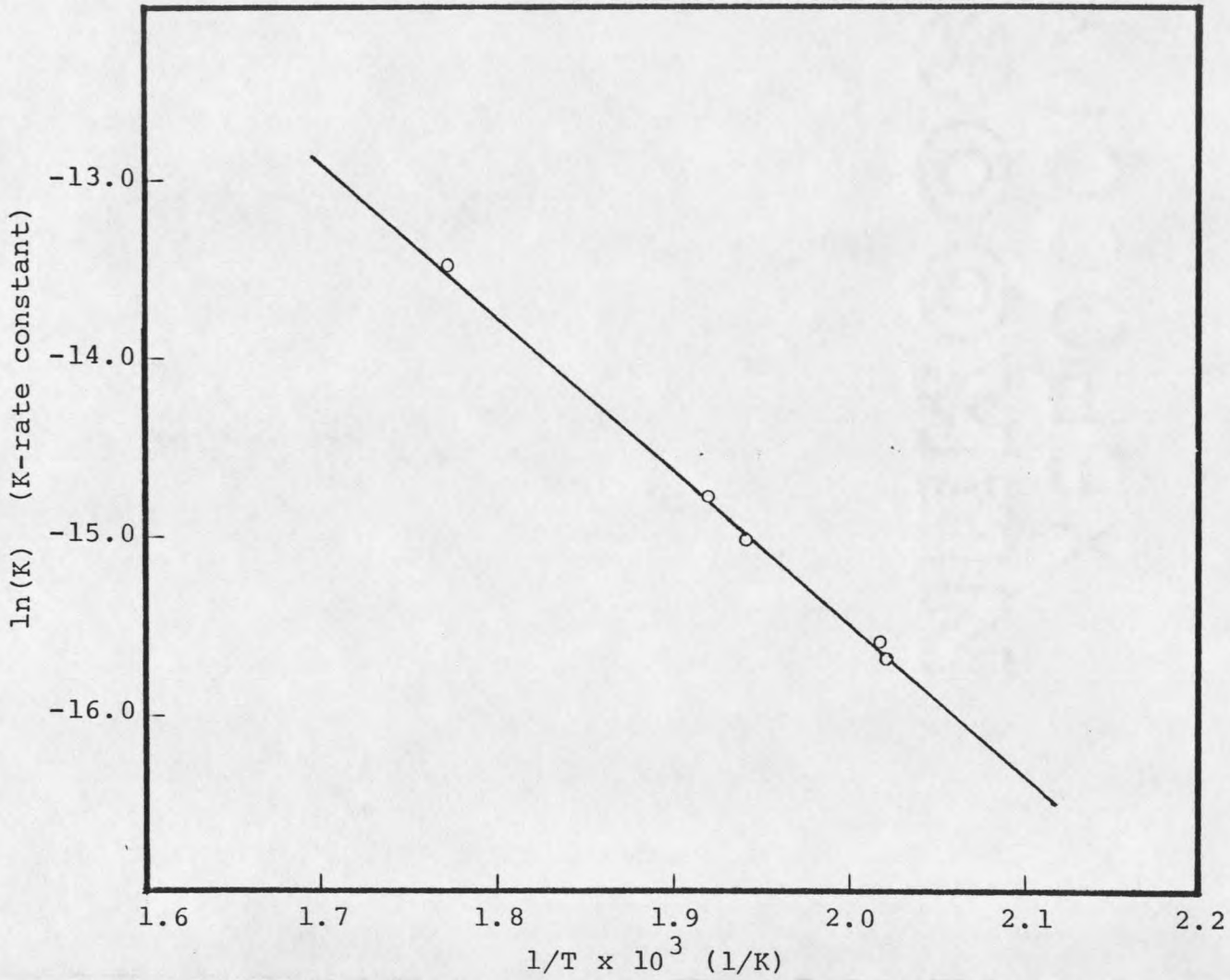

Figure 25. Arrhenius plot for sample A-10 in p-cymene cracking reaction.

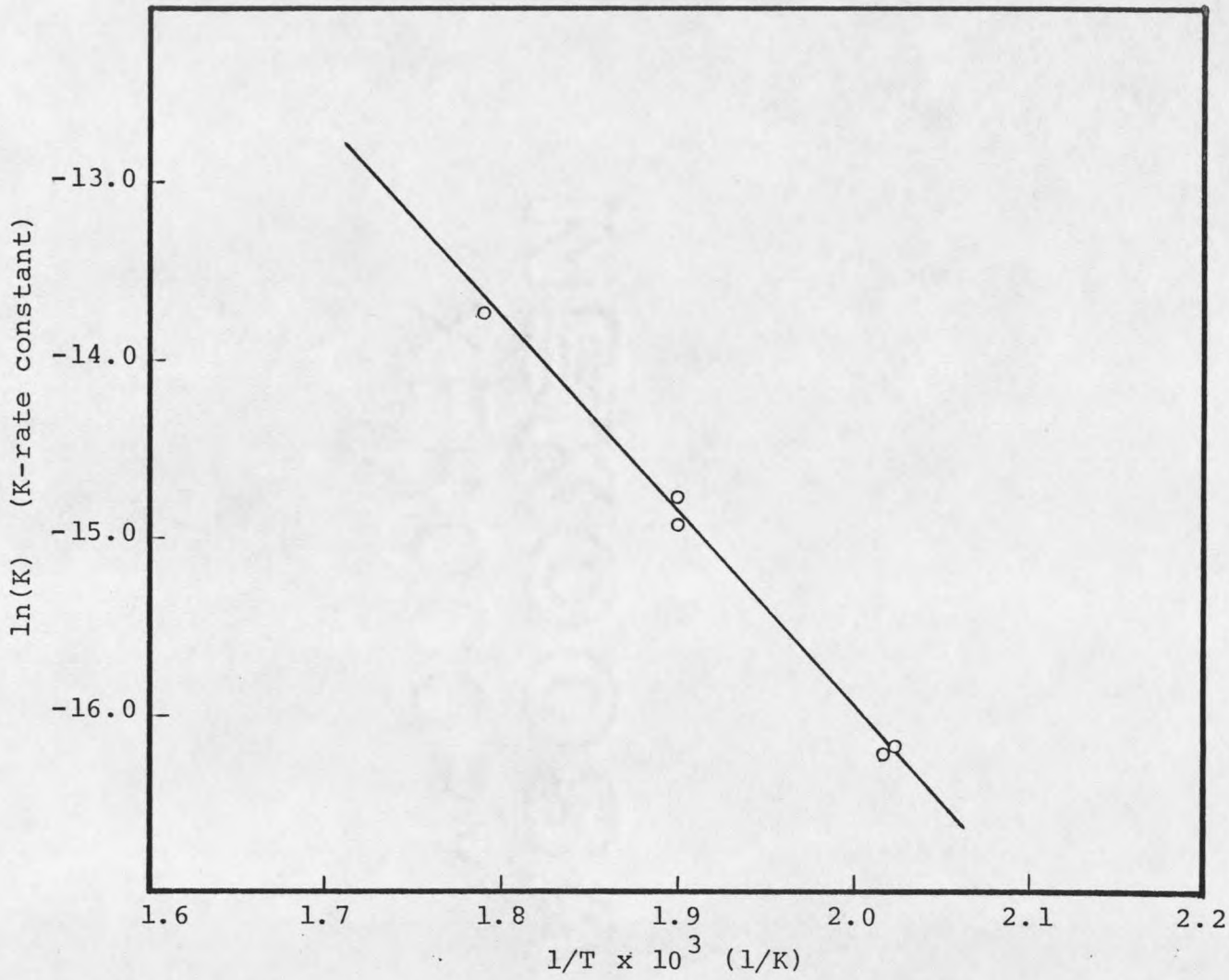

Figure 26. Arrhenius plot for sample A-44 in p-cymene cracking reaction.

for p-cymene cracking. The observed activation energies are listed in Table 9. The activation energies for o-xylene isomerization which were from J. Golden's work [9] are also listed in this table.

Table 9. Activation Energy Comparison.

sample	p-cymene cracking E_a (kcal/mole)	o-xylene isomerization E_a (kcal/mole)
A-3	ND	22.0
A-7	ND	21.2
A-10	15.9	16.0
A-18	ND	22.1
A-26	ND	16.2
A-44	19.1	19.8
A-65	0	0
A-88	ND	ND
A-100	ND	ND

ND: Not determined.

Comparing the E_a values for samples A-10 and A-44, it is obvious that for the same alumina-content catalyst, p-cymene cracking and o-xylene isomerization possess almost the same activation energy. A suggestion can be made from the E_a-equality that p-cymene cracking reaction and o-xylene isomerization may occur on the same kind of active sites. As discussed before, both the cracking reaction and isomerization are carbonium-ion reactions and they both

relate to Bronsted acid sites. Thus they may proceed the same steps in the reaction: reactant adsorption on active sites; carbonium ion formation; reaction of carbonium ions; and desorption of product from active sites of the catalysts. One of these steps must be a rate-controlling step. Since p-cymene cracking reaction and o-xylene isomerization have very close values of activation energies and the same pattern of reaction rate constant, it is possible to conclude that these two reactions have the same kind of reaction mechanism and the same rate-controlling step.

Kinetics and Mechanism Study For P-cymene Cracking

Kinetics Study

As introduced before, the rate constant k for p-cymene cracking was calculated based on the assumption of first order reaction. However, it is not clear what order reaction it is for p-cymene cracking. From the experimental data, which are shown through Fig. 30 to Fig. 35, the first and second peaks (which represent the products of light hydrocarbons and toluene respectively) show a higher activity at the beginning of the reaction and then, after 45 minutes of transient time, the activity falls to a steady value. If p-cymene cracking was a first order reaction, the reaction rate should be proportional to the p-cymene

concentration inside of the reactor. This phenomenon indicates that the reaction rate of p-cymene cracking is not proportional to p-cymene concentration since the p-cymene concentration increased to a steady value in ~40 minutes (which is 5 × residence time).

Cortes Arroyo et al. studied the kinetics and mechanism of p-cymene cracking on silica-alumina catalysts at 425 ^{0}C [30] in which they found that propane and toluene were the cracking products and other products did not exceed 2% of the main products. From the experimental data they concluded that the reactant p-cymene and the products were both adsorbed on the active sites of the catalysts, the active centers were all the same kind, and the rate determining step was the surface reaction.

The following is an analysis of the transients found in p-cymene cracking reaction based on the mechanism of Cortes Arroyo et al.

The overall reaction of p-cymene cracking can be represented as:

A = B + C

where A ---- reactant p-cymene

B ---- product propane

C ---- product toluene

A is adsorbed on an active center X_1, which forms a complex with A. Since two molecules B and C are produced from each A molecule that reacts and B and C are both

adsorbed, it is necessary for an empty site X_2 to be present adjacent to the reacting molecule (A) to accommodate one of the product molecules. In a general way the process is written as:

$$A + X_1 = A \cdot X_1 \qquad \text{(adsorption)}$$

$$A \cdot X_1 + X_2 = B \cdot X_2 + C \cdot X_1 \qquad \text{(reaction)}$$

$$B \cdot X_2 + C \cdot X_1 = B + C + X_1 + X_2 \qquad \text{(desorption)}$$

The fraction of available sites covered with A, B, and C are:

$$Z_A = K_A P_A (1-\Sigma Z)$$

$$Z_B = K_B P_B (1-\Sigma Z)$$

$$Z_C = K_C P_C (1-\Sigma Z)$$

$$(1-\Sigma Z) = 1/(1+K_A P_A+K_B P_B+K_C P_C)$$

where

K_i = equilibrium constant of i for adsorption-desorption

P_i = pressure of i

Based on the surface reaction as a controlling step, the reaction rate equation should be:

$$-r_s = k_s Z_A (1-\Sigma Z) - k_s Z_B Z_C$$

$$= k_s K_A (P_A - P_B P_C / K_s K)/(1+K_A P_A+K_B P_B+K_C P_C)^2$$

where

k_s = surface reaction rate constant

K_s = equilibrium rate constant of total reaction

K = equilibrium constant for total adsorption-desorption

The experimental data in Fig. 27 and Fig. 28 are used to verify the proposed rate equation above. Fig. 27 represents sample A-10 in p-cymene cracking at 222^0C and the conversion of p-cymene was about 0.1; Fig. 28 represents sample A-44 in the same reaction at 220^0C and the conversion was 0.04. The first peak represents propane, the second peak toluene, and the third peak p-cymene. P-cymene concentration was much larger than those of the products throughout the reaction. With the information above, assumptions about the reaction were made as follows:

(1) Since initially the concentration of p-cymene >> the concentration of products, $K_AP_A >> K_BP_B$ and $K_AP_A >> K_CP_C$, then

$$(1+K_AP_A+K_BP_B+K_CP_C)^2 = (1+K_AP_A)^2$$

(2) Since the conversion of p-cymene is very small (0.04 - 0.1), P_B and P_C were assumed negligible, then

$$(P_A - P_BP_C/K_SK) = P_A$$

The rate equation is then simplified as

$$-r_S = k_SK_AP_A/(1+K_AP_A)^2$$

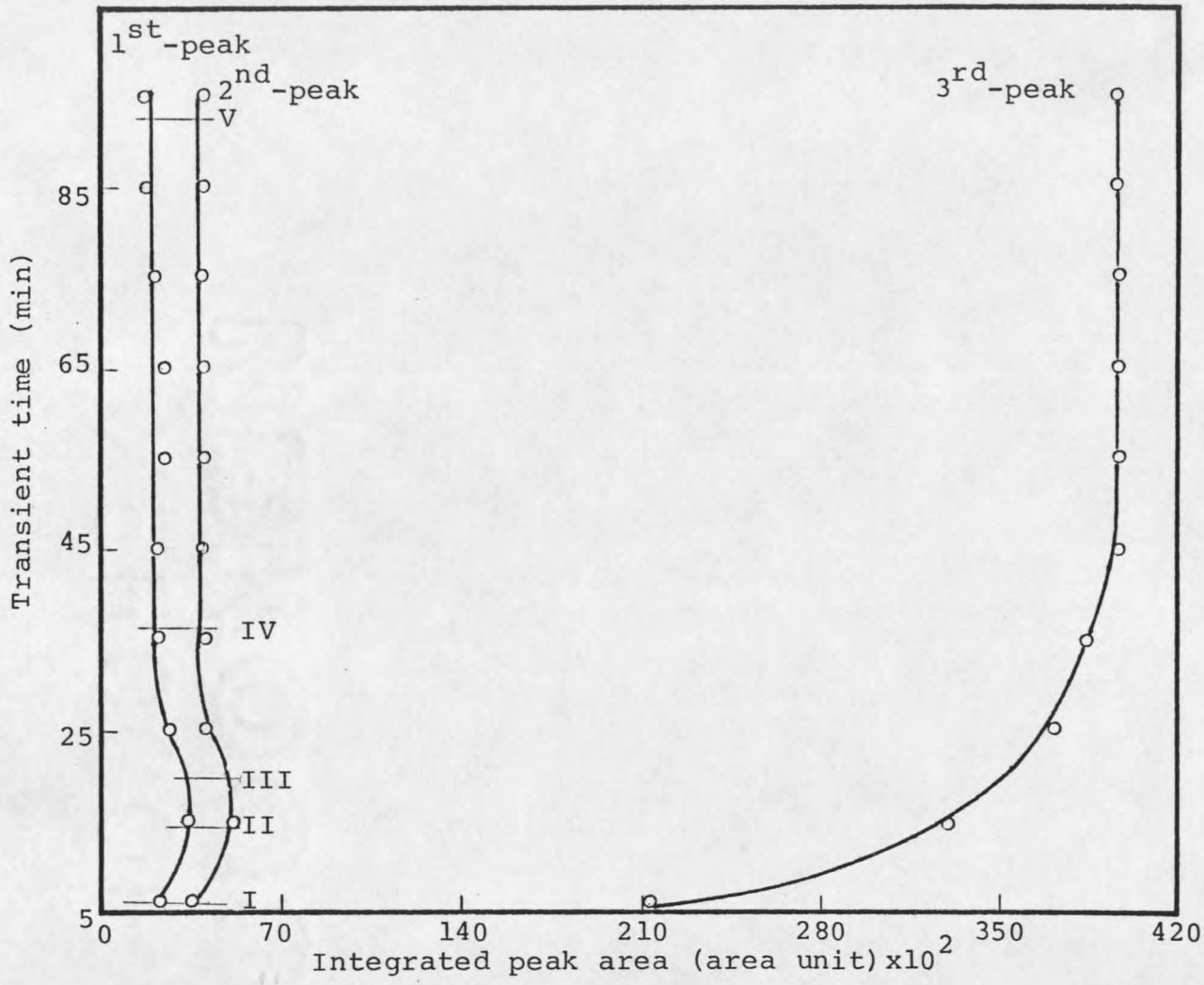

Figure 27. Experimental data for sample A-10 in p-cymene cracking reaction at 222°C.

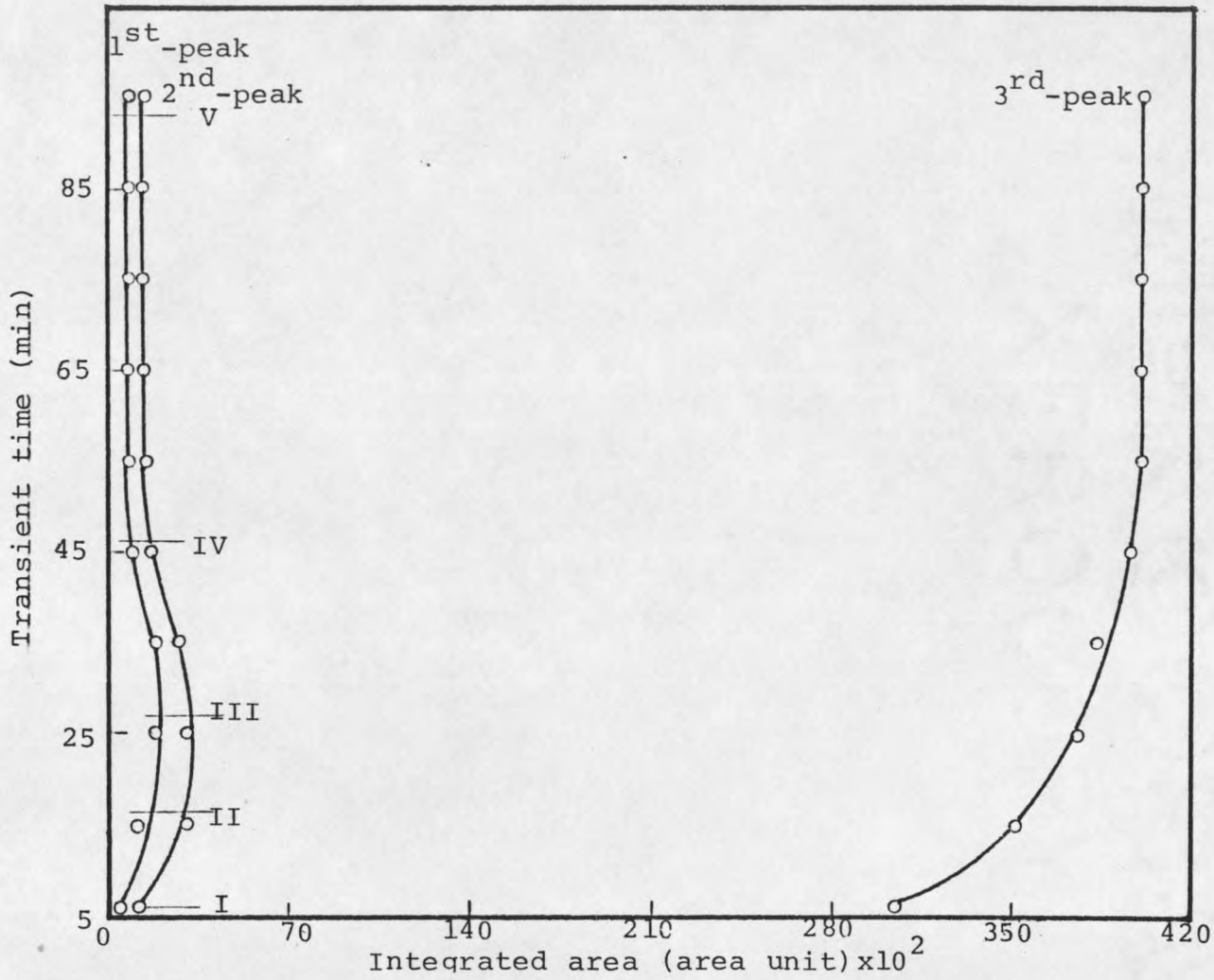

Figure 28. Experimental data for sample A-44 in p-cymene cracking reaction at 220°C.

As mentioned before, p-cymene concentration was increased from zero to a steady value. At very beginning of the reaction, the concentration of p-cymene is very small and $K_A P_A << 1$, then

$$(1 + K_A P_A)^2 = 1$$

$$-r_S = k_S K_A P_A \qquad \text{(Equation 1)}$$

The reaction rate is increased with the increasing p-cymene concentration and shows 1st order initially. Later, p-cymene concentration becomes larger and $K_A P_A \geqslant 1$, (and there is some distribution from $K_B P_B$, $K_C P_C$), then

$$-r_S = k_S K_A P_A / (1 + K_A P_A + K_B P_B + K_C P_C)^2 \qquad \text{(Equation 2)}$$

The reaction rate is no longer 1st order, but still generally follows the p-cymene concentration. It levels off with the level of steady state concentration of p-cymene. The slight decrease can be explained by the kinetic adsorption effect of A, B, and C, plus the lag time for the diffusion into and out of the pellets.

The experimental data in Fig. 27 and Fig. 28 have good agreements with the rate changes discussed above where the region I-II shows a increasing rate at low p-cymene concentration and it follows Eq. (1); the region III-VI shows a decreasing rate at high p-cymene concentration and

it follows Eq. (2); in the region IV-V, the transient time is longer than 45 minutes, the concentration of p-cymene no longer changes, so the reaction rate remains constant. The proposed kinetic equation for p-cymene cracking is reasonable.

Mechanism Study

The mechanism study for p-cymene cracking reaction is presented basically in terms of the product distribution. As can be seen in Fig. 30 to Fig. 35 and Table 7, when the temperature is near 300^0C, only C_3 saturated hydrocarbons and a C_7 fraction, which is toluene, appear as products in p-cymene cracking. The reactions over the temperature range 220-320^0C displayed the same product distribution (Fig. 27 and Fig. 28).

Bronsted acid sites have been shown to be very active for p-cymene cracking reaction. Moreover, from Table 4 [22], catalytic cracking yields fractions which are uniformly distributed over C_3 (C_3H_8), C_7 (toluene), and C_{10} (unreacted p-cymene) while only at high temperature do C_8, C_9 and other fractions form. The p-cymene mechanism proposed is then: p-cymene adsorbs on a Bronsted active site to form an intermediate substance, it then cracks to provide final products, and products desorb from the catalysts to allow further reaction. Dual sites are required for p-cymene cracking because there are two molecules of products formed out of every one p-cymene molecule and both products are

absorbed on the active sites. Thus another free active site is needed which should be close to the reacted site.

The probable steps of cracking are outlined as follows:

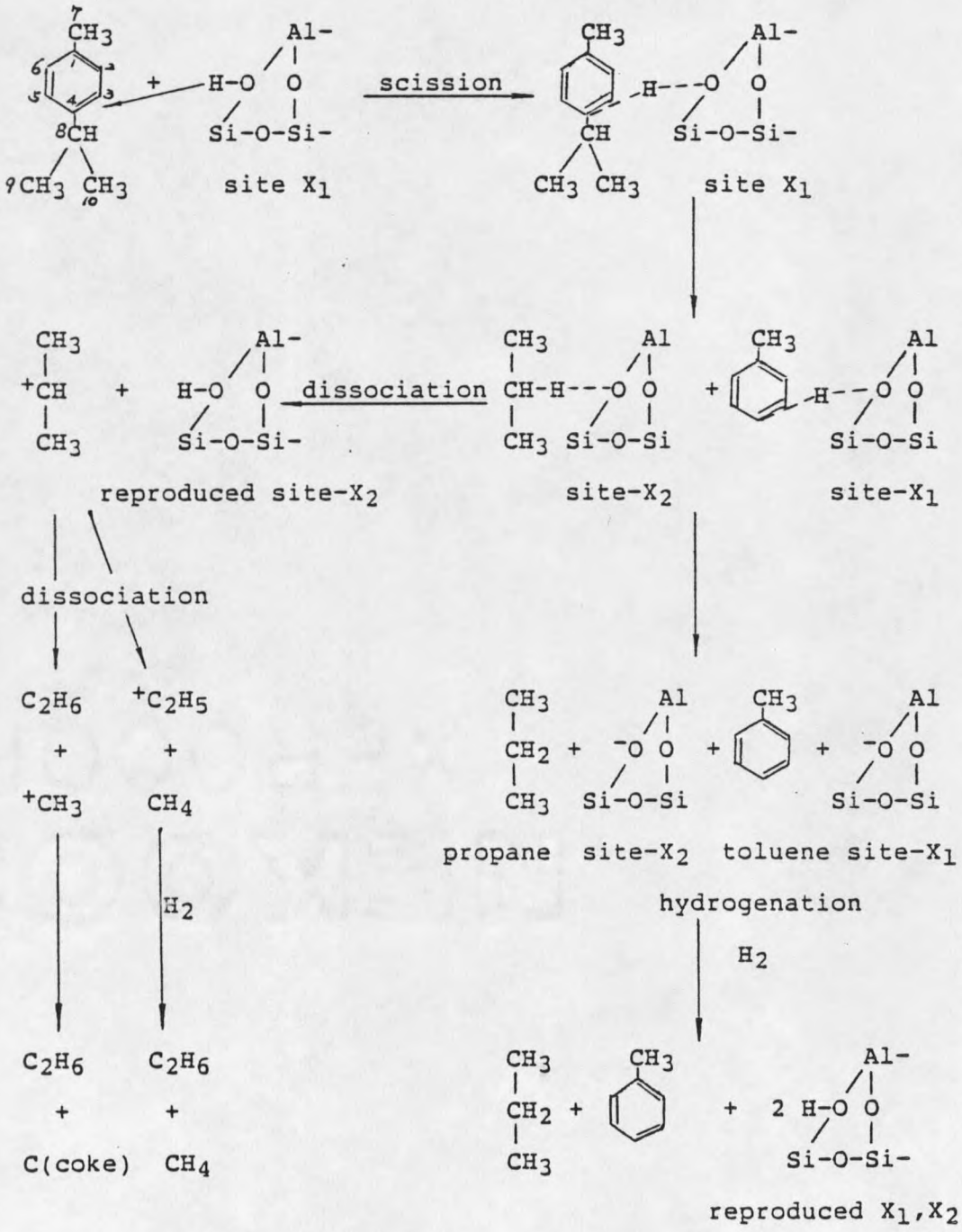

Aromatic hydrocarbons stabilize by scission at the carbon No. 4 position to become a carbonium ion. The production of toluene can be explained by the scission of the ring between No. 4 and No. 8 carbon atoms, the latter being the carbonium carbon. With the presence of hydrogen in the reaction, the propyl carbonium ion is easily hydrogenated to propane. Propylene formation is not likely because of the hydrogen presence. There is a possibility for methane and ethane formation and it is due to the dissociation of propyl radical. Those products are in a very small amount (not detectable). The coke formation on the catalyst surfaces can be explained by heavy cracking of methyl and benzyl radicals, which turn to carbon.

The product distribution here is almost the same as that in thermal cracking where the major products are toluene and saturated hydrocarbons. A free radical mechanism proved to dominate thermal cracking [24]. It is possible, but unlikely, that a radical mechanism partially participates in the p-cymene cracking. With the existing catalysts and relatively low temperature, this catalytic cracking reaction is thought to be influenced by the carbonium ion mechanism and not the radical mechanism.

The question arises as to why the scission dose not happen at carbon No.1 position. Usually it is the heavier side chain that splits more easily than the shorter one. In p-cymene cracking reaction, the propyl carbonium ion is

easier to form than the methyl carbonium ion because the tertiary carbonium ion is more stable than the primary carbonium ion. Moreover, a propyl group will first split off the benzene ring because of steric effects.

CONCLUSIONS

1. The catalytic activity for p-cymene cracking is proportional to Bronsted-acidity for low-alumina-content catalysts. Bronsted acid sites are active sites and directly provide activity to the cracking reaction.

2. The activation energies for p-cymene cracking are close to those for o-xylene isomerization and they have the same pattern with respect to alumina contents and the value of rate constants. The two reactions appear to have a similar carbonium-ion mechanism and may be catalyzed by the same active sites.

3. It does not appear from the present work that Lewis acid sites participate directly in the cracking reactions. Bronsted acid sites definitely provide activity for both cracking and isomerization. However, Lewis acid sites can make Bronsted acid sites more active.

REFERENCES CITED

1. Gates, B.C., Katzer, J.R., and Schuit, G.C.A., Chemistry of Catalytic Processes, McGraw-Hill, NY (1979).

2. Parry, E.P., "Infrared Study of Pyridine Adsorbed On Acidic Solids. Characterization of Surface Acidity", J. Catal., 2, 371 (1963).

3. Pines, H., and Haag, W.O., "Alumina: Catalyst and Support. 1. Alumina, Its Intrinsic Acidity and Catalytic Activity", J. Am. Chem. Soc., 82, 2471 (1960).

4. Ward, J.W., "The Nature of Active Sites on Zeolites. XI. The Effects of The Silica-to-Alumina Ratio on The Acidity and Catalytic Activity of Synthetic Faujasite-Type Zeolites", J. Catal., 17, 355 (1970).

5. Chapman, J.E., and Hair, M.L., "The Role of The Surface Hydroxyl Groups In Catalytic Cracking", J. Catal., 2, 145 (1963).

6. Hall, W.K., Lutinski, F.E., and Gerberich, H.R., "Studies of The Hydrogen Held by Solids. VI. The Hydroxyl Groups of Alumina and Silica-Alumina as Catalytic Sites", J. Catal., 3, 512 (1964)

7. Fedorynska, E., Wozniewski, T., Malnislaw, S., and Ahmed, I., J. Coll. and. Int. Sci., "Investigation of Physico-chemical and Catalyst Properties of Silica-alumina Gels", 69, 469 (1979).

8. Saṭo, M., Kanbayashi, T., Kobayashi, N., and Shima, Y., "Hydroxyl Groups On Silica, Alumina, and Silica-Alumina Catalysts", J. Catal. 7, 342 (1967).

9. Golden, J.L., "Acidity and O-xylene Isomerization of Silica-Alumina Catalysts", Ph. D Thesis, Montana State University (1986).

10. Hendrickson, J.B., Cram, D.J., and Hammond, G.S., Organic Chemistry, 3rd Ed., McGraw-Hill, NY (1970).

11. Mapes, J.E., and Eischens, R.P., "The Infrared Spectra of Ammonia Chemisorbed on Cracking Catalysts", J. Phys. Chem., 58, 1059 (1954).

12. Basila, M.R., and Kantner, T.R., "The Infrared Spectrum of Ammonia Adsorbed on Silica-Alumina", J. Phys. Chem., 71, 467 (1967).

13. Bourne, K.H., Cannings, F.A., and Pitkethly, R.C., "The Structure and Properties of Acid Sites in a Mixed-Oxide System I. SyntBesis and Infrared Characterization", J. Phys. Chem., 74, 2197 (1970).

14. Schwarz, J.A., "Simultaneous Determination of Lewis and Bronsted Site Densities on Silica-Alumina Using Infrared Techniques", J. Vac. Sci. Technol., 12, 321 (1975).

15. Gay, I.D., and Liand, S., "Investigation of Surface Acidity by ^{13}C-NMR Adsorption of Amines on Silica, Alumina, and Mixed Silica-Alumina", J. Catal. 44, 306 (1976).

16. Bermer, V.H., Slinberg, K.H., and Chuong, T.K., "The Influence of Alkali Contamination of The Surface Chemical Properties of Amorphous Silica-Alumina Catalysts", Z. Anorg. Allg. Chem., 400, 115 (1973).

17. Leonard, A.J., Ratnasamy, P., Declerek, F.D., and Fripiat, J.J., "Structure and Properties of Amorphous Silica-Alumina Part 5. Nature and Properties of Silica-Alumina Surfaces", Discuss. Faraday Soc., 52, 98 (1971).

18. Holm. V.C.F., and Clark, A., "Cracking of N-octane, Polymerization of Propylene, O-xylene Isomerization, Hydrogen Transfer, and H-D Exchange", J.Catal., 2, 16-20 (1963).

19. Holm, V.C.F., Bailey, G.C., and Clark, A., "Acidity Studies of Silica-Alumina Catalysts", J. Phys. Chem., 63, 129 (1959).

20. Clark, A., Holm, V.C.F., and Blackburn, D.M., "Thermodynamics of Adsorption of Ammonia", J. Catal., 1, 244 (1962).

21. Sato, M., Aonuma, T., and Shiba, T., Proc. 3rd Int. Cong. Catal., P. 396, North-Holland, Amsterdam, (1965).

22. Janardha[B P.B., and Rajeswari, S., "Silica-Alumina Gel Behavior as Cracking Catalyst", Ind. Eng. Chem. Prod. Res. Dev., 16, 52 (1977).

23. Hightower, J.W., Emmett, P.H., Proc. Int. Cong. Catal., 3rd Amsterdam, 1, 688-196 (1964).

24. Greensfelder, B.S., Voge, H.H., Good, G.M., Ind. Eng. Chem., 41, 2573 (1949).

25. Hansford, R.C., Ind. Eng. Chem., 39, 849 (1947).

26. Hindin, S.G., Mills, G.A., and Oblad, A.G., "Hydrogen Exchange Between Cracking Catalysts and Butanes", J. Am. Chem. Soc., 73, 278 (1951).

27. Sedran, U.A., Figoli, N.S.,"Relation Between Acidity and Activity During the Transformation of Methanol Into Hydrocarbons on Amorphous Silica-alumina", Appl. Catal., 19, 317-325 (1985)

28. Hansford, R.C. and Ward, J.W., "The Nature of Active sites on Zeoletes VII., Relative Activities of Crystalline and Amorphous Alumino-Silicates", J.Catal., 13, 316 (1969)

29. Matsumoso, H., Take, J.I., and Yoneda, Y., "Linear Free Energy Relationships in Heterogeneous Catalysts VIII. Isomerization of Alkylbenzenes Over Solid Acid Catalysts", J. Catal., 11, 221-219 (1968)

30. Cortes Arroyo, A., Garcia de la Banda, J. F., and Hermana Tezanos, E., "Kinetics and Mechanism of Cracking of P-cymene On Silica-Alumina Catalysts", An Real Soc. Espan. Fis. Quim., Ser. 13, 63(9-10), 847-856 (1967)

APPENDIX

Table 10. Peak Areas From P-cymene Cracking At 315°C*.

sample	1st-peak area	2nd-peak area	3rd-peak area	input-peak area	p-cymene conversion
A-3	13000	17500	29000	48700	0.4045
A-7	12500	16500	27200	46800	0.4188
A-10	14500	19500	26800	49800	0.4618
A-18	11500	16000	34750	51700	0.3279
A-26	13750	18250	32750	54700	0.4013
A-44	12500	16500	34750	53900	0.3553
A-65	0	0	48000	48000	0
A-88	ND	-	-	-	-
A-100	ND	-	-	-	-

* Data are those after 45 minutes of transient time.

Table 11. Activity Calculation For P-cymene Cracking At Unchanged Temperature:

sample	reaction temp. (^{o}C)	catalyst weight (g)	surface area (m^2)	mass flow rate (g-cymene/s)	p-cymene conversion X	$\frac{X}{1-X}$	reaction rate (mol/s·m^2)	rate constant (l/s)
A-3	315	0.0955	40.68	$4.00x10^{-5}$	0.4045	0.6793	$3.06x10^{-9}$	$2.68x10^{-4}$
A-7	315	0.1115	37.67	$4.23x10^{-5}$	0.4188	0.7206	$3.50x10^{-9}$	$2.73x10^{-4}$
A-10	315	0.1232	35.11	$4.51x10^{-5}$	0.4618	0.8580	$4.42x10^{-9}$	$2.89x10^{-4}$
A-18	315	0.1145	15.08	$4.67x10^{-5}$	0.3279	0.4879	$7.57x10^{-9}$	$1.99x10^{-4}$
A-26	315	0.1155	20.10	$4.95x10^{-5}$	0.4013	0.6703	$7.37x10^{-9}$	$2.87x10^{-4}$
A-44	315	0.1214	24.04	$4.88x10^{-5}$	0.3553	0.5511	$5.36x10^{-9}$	$2.11x10^{-4}$
A-65	315	0.1415	0.98	$4.34x10^{-5}$	0	0	0	0
A-88	ND	-	-	-	-	-	-	-
A-100	ND	-	-	-	-	-	-	-

Table 12. P-cymene Cracking Activity Data For Sample A-10 At Different Temperature:

run number	reaction temp. (^{o}C)	catalyst weight (g)	surface area (m^2)	mass flow rate (g-cymene/s)	p-cymene conversion X	rate constant k ($mol/s \cdot m^2$)	logarithm of rate constant ln(k)
1	222	0.1100	31.35	4.05×10^{-5}	0.1116	1.622×10^{-9}	-15.63
2	221	0.1274	36.31	4.05×10^{-5}	0.1406	1.825×10^{-9}	-15.52
3	245	0.1166	33.23	3.62×10^{-5}	0.1429	1.825×10^{-9}	-15.52
4	250	0.1202	34.26	4.81×10^{-5}	0.2050	3.622×10^{-9}	-14.83
5	291	0.1069	30.47	4.52×10^{-5}	0.4600	12.85×10^{-9}	-13.56

Table 13. P-cymene Cracking Activity Data For Sample A-44 At Different Temperature:

run number	reaction temp. (^{o}C)	catalyst weight (g)	surface area (m^2)	mass flow rate (g-cymene/s)	p-cymene conversion X	rate constant k ($mol/s \cdot m^2$)	logarithm of rate constant ln(k)
1	218	0.1073	21.27	3.73×10^{-5}	0.0485	0.893×10^{-9}	-16.23
2	220	0.1100	21.78	3.73×10^{-5}	0.0485	0.872×10^{-9}	-16.26
3	252	0.1111	22.0	3.62×10^{-5}	0.1700	3.368×10^{-9}	-14.90
4	252	0.1100	21.78	3.62×10^{-5}	0.1750	3.523×10^{-9}	-14.68
5	288	0.1018	20.15	4.52×10^{-5}	0.3300	11.05×10^{-9}	-13.72

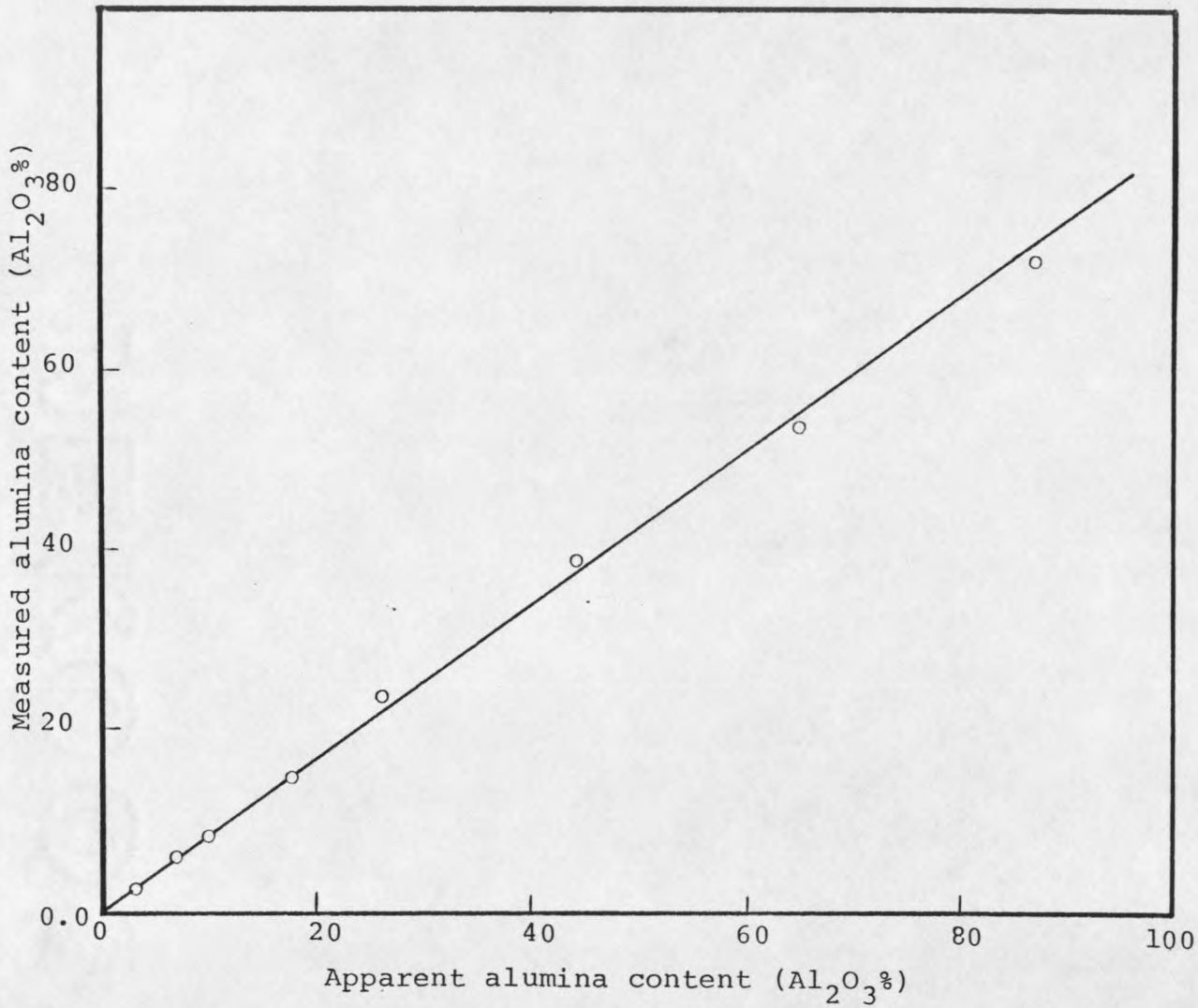

Figure 29. The conversion of apparent and measured alumina contents in silica-alumina catalysts.

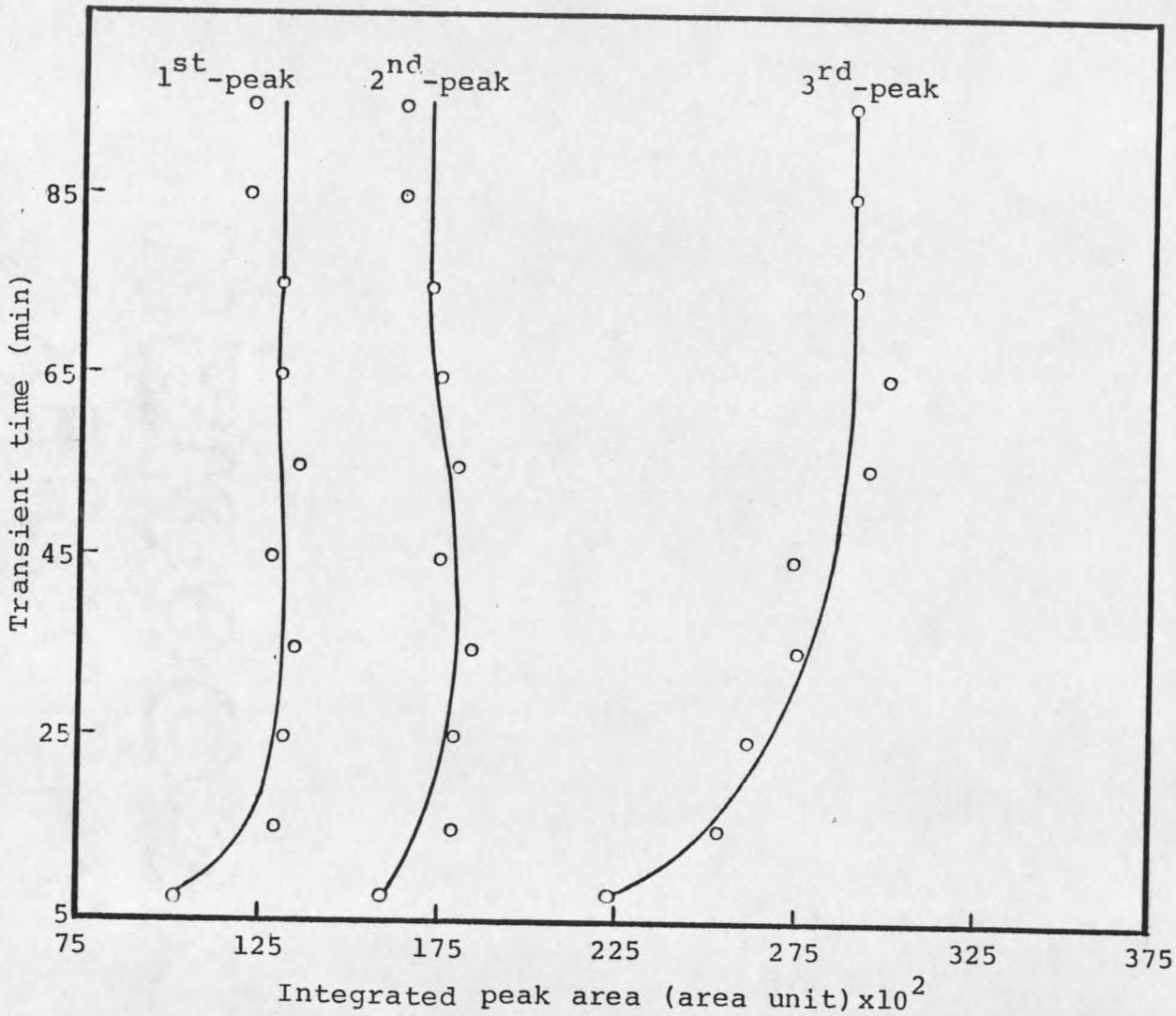

Figure 30. Experimental data for sample A-3 in p-cymene cracking reaction at 315°C.

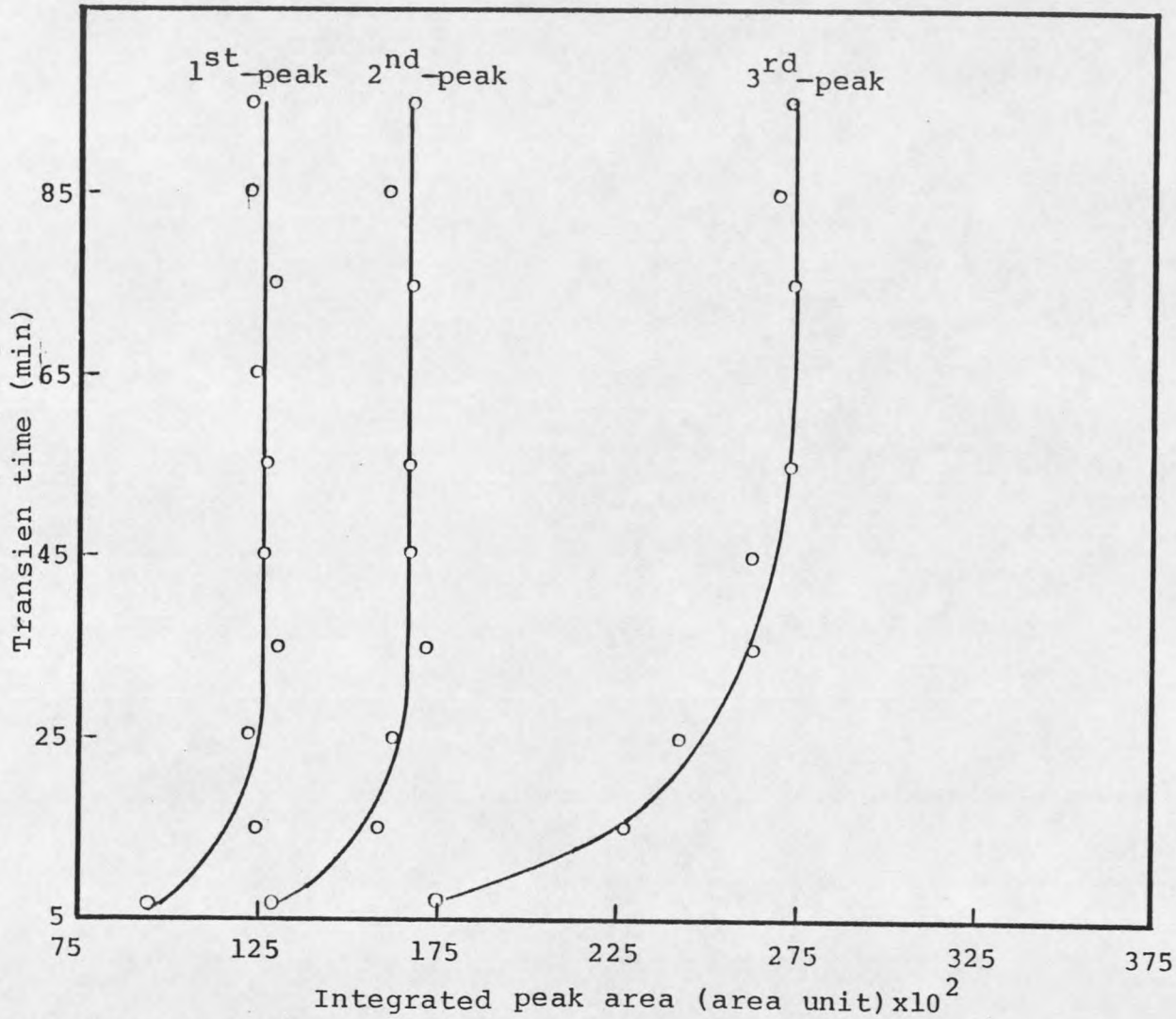

Figure 31. Experimental data for sample A-7 in p-cymene cracking reaction at 315°C.

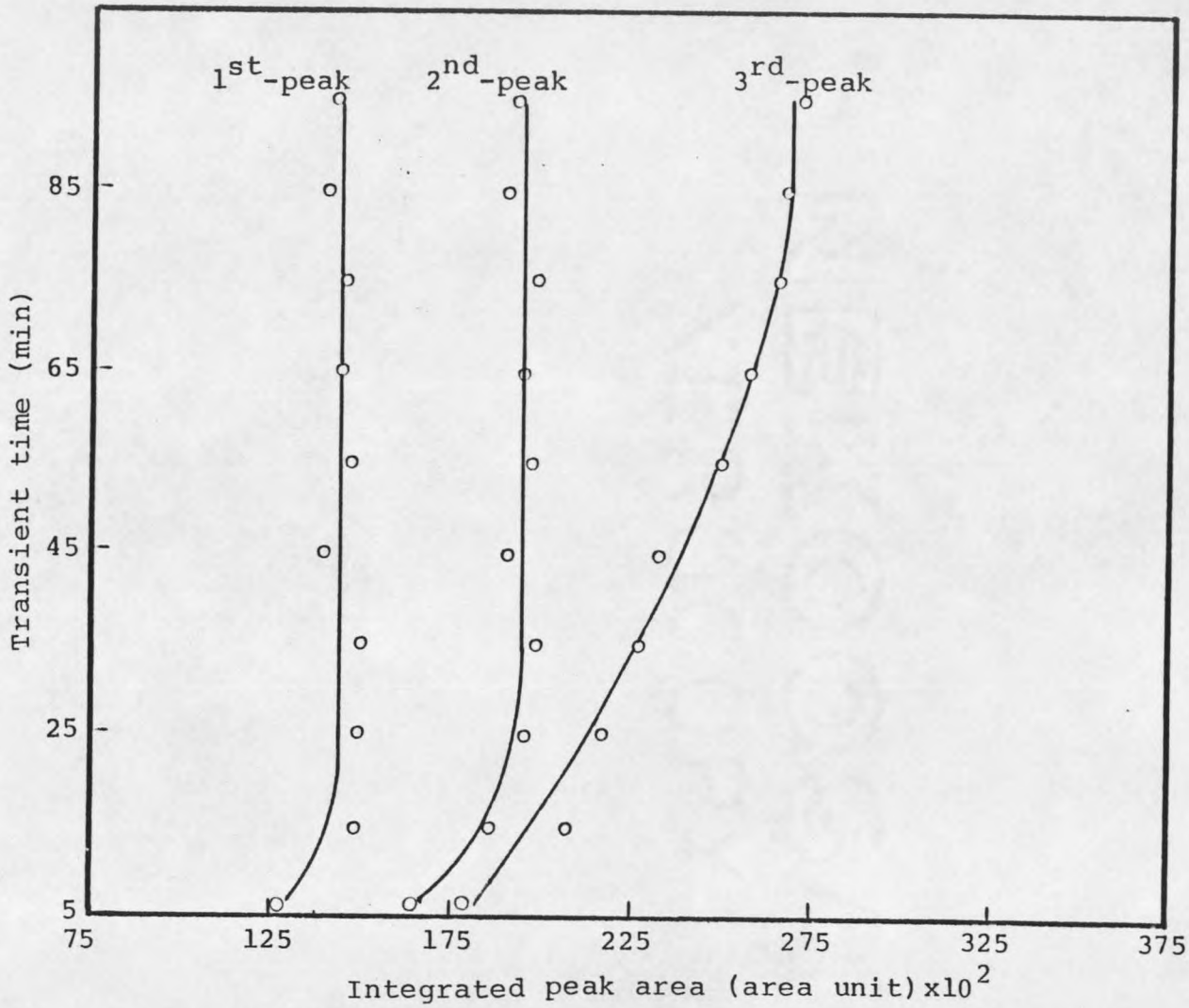

Figure 32. Experimental data for sample A-10 in p-cymene cracking reaction at 315°C.

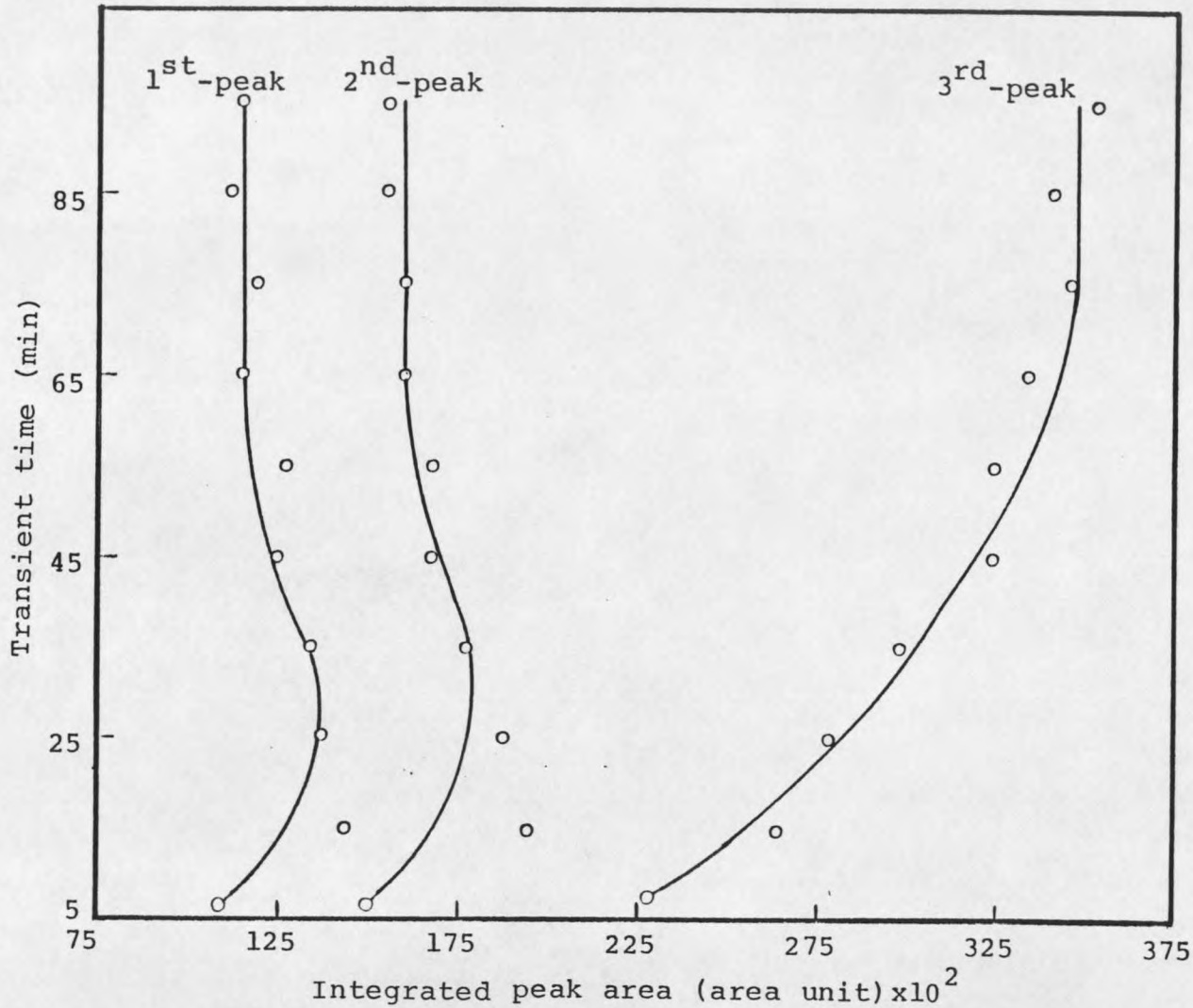

Figure 33. Experimental data for sample A-18 in p-cymene cracking reaction at 315°C.